in photoreceptor cells, creatine supply to photoreceptor cells from local Müller glia might take place in patients with CRT deficiency.

We studied creatine biosynthesis using albino Wistar rats. Although the retina in albino rats is likely stressed by exposing light compared with that in pigmented rats, we do not think that the creatine biosynthesis in the isolated and dark-adapted (i.e., incubated for 24 h under dark) retinas is influenced by light-induced stress. Moreover, Blaszczyk et al. (2004) reported that the concentrations of γ-aminobutyric acid, L-glutamic acid, and L-serine in the isolated retina of pigmented Long Evans rats are not very largely different from those found in albino Wistar rats.

We provide evidence, for the first time, that creatine is preferentially biosynthesized in Müller cells of the retina. Our current and previous findings offer important information that will increase our understanding of the mechanism of creatine supply and creatine kinetics in the retina and of creatine supplementation in patients with creatine deficiency syndromes.

ACKNOWLEDGMENTS

The authors thank Dr. K. Katayama (Toyama Medical and Pharmaceutical University) for valuable discussions and Dr. D. Jack and Dr. K.J. Kim (University of Southern California) for critical reading of the manuscript. This study was supported, in part, by a Grant-in-Aid for Scientific Research from the Japan Society for the Promotion of Science and a grant for Research on Sensory and Communicative Disorders by the Ministry of Health, Labor, and Welfare, Japan.

REFERENCES

Blaszczyk WM, Straub H, Distler C. 2004. GABA content in the retina of pigmented and albino rats. NeuroReport 15:1141–1144.

Defalco AJ, Davies RK. 1961. The synthesis of creatine by the brain of the intact rat. J Neurochem 7:308–312.

Dringen R, Verleysdonk S, Hamprecht B, Willker W, Leibfritz D, Brand A. 1998. Metabolism of glycine in primary astroglial cells: synthesis of creatine, serine, and glutathione. J Neurochem 70:835–840.

Gadea A, Lopez E, Lopez-Colome AM. 1999. Characterization of glycine transport in cultured Müller glial cells from the retina. Glia 26:273–279.

Hall SW, Kühn H. 1986. Purification and properties of guanylate kinase from bovine retinas and rod outer segments. Eur J Biochem 161:551–556.

Hosoya K, Tomi M. 2005. Advances in the cell biology of transport via the inner blood-retinal barrier: establishment of cell lines and transport functions. Biol Pharm Bull 28:1–8.

Izumi Y, Benz AM, Kurby CO, Labruyere J, Zorumski CF, Price MT, Olney JW. 1995. An ex vivo rat retinal preparation for excitotoxicity studies. J Neurosci Methods 60:219–225.

Jones EM. 1995. Na^+- and Cl^--dependent neurotransmitter transporters in bovine retina: identification and localization by in situ hybridization histochemistry. Vis Neurosci 12:1135–1142.

Koenekoop RK. 2004. An overview of Leber congenital amaurosis: a model to understand human retinal development. Surv Ophthalmol 49:379–398.

Magistretti PJ, Pellerin L, Rothman DL, Shulman RG. 1999. Energy on demand. Science 283:496–497.

Mardashchev SR. 1975. Guanidinoacetate-N-methyltransferase: location in mammalian retina and rat Harderian gland. Biokhimiia 40:353–357.

Nakashima T, Tomi M, Katayama K, Tachikawa M, Watanabe M, Terasaki T, Hosoya K. 2004. Blood-to-retina transport of creatine via creatine transporter (CRT) at the rat inner blood-retinal barrier. J Neurochem 89:1454–1461.

Pfeiffer-Guglielmi B, Francke M, Reichenbach A, Fleckenstein B, Jung G, Hamprecht B. 2004. Glycogen phosphorylase isozyme pattern in mammalian retinal Müller (glial) cells and in astrocytes of retina and optic nerve. Glia 49:84–95.

Poitry-Yamate CL, Poitry S, Tsacopoulos M. 1995. Lactate released by Müller glial cells is metabolized by photoreceptors from mammalian retina. J Neurosci 15:5179–5191.

Pow DV, Crook DK. 1997. Immunocytochemical analysis of the transport of arginine analogues into nitrergic neurons and other cells in the retina and pituitary. Cell Tissue Res 290:501–514.

Reye P, Penfold P, Pow DV. 2001. Glyt-1 expression in cultured human Müller cells and intact retinae. Glia 34:311–315.

Rauen T, Wiessner M. 2000. Fine tuning of glutamate uptake and degradation in glial cells: common transcriptional regulation of GLAST1 and GS. Neurochem Int 37:179–189.

Sather WA, Detwiler PB. 1987. Intracellular biochemical manipulation of phototransduction in detached rod outer segments. Proc Natl Acad Sci USA 84:9290–9294.

Schulze A. 2003. Creatine deficiency syndromes. Mol Cell Biochem 244:143–150.

Shen F, Chen B, Danias J, Lee KC, Lee H, Su Y, Podos SM, Mittag TW. 2004. Glutamate-induced glutamine synthetase expression in retinal Müller cells after short-term ocular hypertension in the rat. Invest Ophthalmol Vis Sci 45:3107–3112.

Sipila I, Simell O, Arjomaa P. 1980. Gyrate atrophy of the choroid and retina with hyperornithinemia. Deficient formation of guanidinoacetic acid from arginine. J Clin Invest 66:684–687.

Sipila I, Valle D, Brusilow S. 1992. Low guanidinoacetic acid and creatine concentration in gyrate atrophy of the choroids and retina (GA). In: De Deyn PP, Marescau B, Stalon V, Qureshi IA, editors. Guanidino compounds in biology and medicine. London: John Libbey. p 379–383.

Tachikawa M, Fukaya M, Terasaki T, Ohtsuki S, Watanabe M. 2004. Distinct cellular expressions of creatine synthetic enzyme GAMT and creatine kinases uCK-Mi and CK-B suggest a novel neuron-glial relationship for brain energy homeostasis. Eur J Neurosci 20:144–160.

Tomi M, Funaki T, Abukawa H, Katayama K, Kondo T, Ohtsuki S, Ueda M, Obinata M, Terasaki T, Hosoya K. 2003. Expression and regulation of L-cystine transporter, system xc^-, in the newly developed rat retinal Müller cell line (TR-MUL). Glia 43:208–217.

Wallimann T, Wegmann G, Moser H, Huber R, Eppenberger HM. 1986. High content of creatine kinase in chicken retina: compartmentalized localization of creatine kinase isoenzymes in photoreceptor cells. Proc Natl Acad Sci USA 83:3816–3819.

Wallimann T, Wyss M, Brdiczka D, Nicolay K, Eppenberger HM. 1992. Intracellular compartmentation, structure and function of creatine kinase isoenzymes in tissues with high and fluctuating energy demands: the "phosphocreatine circuit" for cellular energy homeostasis. Biochem J 281:21–40.

Wyss M, Kaddurah-Daouk R. 2000. Creatine and creatinine metabolism. Physiol Rev 80:1107–1213.

Increased JNK Phosphorylation and Oxidative Stress in Response to Increased Glucose Flux through Increased GLUT1 Expression in Rat Retinal Endothelial Cells

Jie Zhou,[1] *Baljit K. Deo,*[1] *Kenichi Hosoya,*[2] *Tetsuya Terasaki,*[3] *Irina G. Obrosova,*[4] *Frank C. Brosius, III,*[1,5,6] *and Arno K. Kumagai*[1,6]

Purpose. To investigate whether increased glucose flux through increased glucose transporter1 (GLUT1) expression results in increased oxidative stress and increased c-jun N-terminal kinase (JNK) phosphorylation.

Methods. GLUT1-overexpressing cells were established using a rat retinal endothelial cell line. The intracellular reactive oxygen species was detected by the oxidation of 5- (and -6)-chloromethyl-2',7'-dichlorodihydrofluorescein diacetate, acetyl ester (CM-H2-DCFDA). Western blot was performed to determine JNK phosphorylation and lipid peroxidation. Differentially expressed genes were detected by cDNA microarray analysis and confirmed by Northern blot analysis.

Results. Clones overexpressing GLUT1 showed an approximate four- to eightfold increase in GLUT1 expression and a 44% increase in intracellular glucose concentrations. GLUT1-overexpressing cells had a 80% increase in DCF fluorescence and increased lipid peroxidation, as well as increased JNK phosphorylation. Analysis of differentially expressed genes in GLUT1-overexpressing cells showed increased expression of JNK interacting protein (JIP)-1, a scaffold protein necessary for JNK activation. Northern blot analysis confirmed upregulation of JIP-1. Immunoprecipitation showed that phosphorylated JNK, but not total JNK, coimmunoprecipitated with JIP-1 protein. At the cellular level, JIP-1 was predominantly localized in cytoplasm, especially in the perinuclear area in retinal endothelial cells.

Conclusions. GLUT1 overexpression and increased glucose flux result in increased oxidative stress and JNK phosphorylation in immortalized rat retinal endothelial cells. Further studies are needed to understand molecular events after increased glucose flux in retinal endothelial cells and the relation between increased oxidative stress and JNK phosphorylation. (*Invest Ophthalmol Vis Sci.* 2005;46:3403–3410) DOI:10.1167/iovs.04-1064

Diabetic retinopathy (DR), a microvascular complication of diabetes mellitus, is one of the leading causes of adult blindness in developed countries. Despite its prevalence and severity, the molecular mechanisms underlying DR have not been fully elucidated. Various mechanisms have been proposed, such as increased flux through polyol[1] and hexosamine pathways,[2,3] nonenzymatic glycosylation, increased formation of advanced glycation end products (AGEs),[4,5] protein kinase C activation,[6] glucose-induced DNA damage,[7] and oxidative stress.[8] All these pathologic changes appear to be initiated by chronic exposure of the retinal microvasculature to increased blood glucose concentrations. Clinical studies have demonstrated a strong association between long-term glycemic control and the development and progression of diabetic retinopathy.[9–12] On a cellular level, prolonged hyperglycemia associated with diabetes mellitus is deleterious to the retinal microvasculature and results in endothelial cell and pericyte death; formation of microaneurysms and acellular capillaries; thickening of basement membranes; and, in severe cases, retinal neovascularization.[13]

Glucose is the major energy source for the retina, and its transport from the blood to the neuroretina is mediated by a facilitative, sodium-independent glucose transporter known as GLUT1.[14–16] The transport of glucose into the retina by GLUT1 exceeds its phosphorylation by hexokinase, the rate-limiting step in retinal glucose metabolism.[17,18] Consequently, measurable free glucose is available as a substrate for biochemical processes thought to be responsible for the development of DR. It is also possible, however, that the effects of elevated glucose concentrations may be mediated by the binding of AGEs to endothelial cell surface receptors (RAGE).[19] Binding of AGE to its receptors has been shown to result in activation of specific signaling pathways,[20] as well as increased oxidative stress[21] and apoptosis[22,23] in vascular cells.

The c-Jun N-terminal kinase pathway is important in modulating cellular responses to stress. Increased oxidative stress has been implicated in several animal models of diabetes through activation of the c-Jun N-terminal kinase, such as β-cell dysfunction and the formation of coronary atherosclerosis.[24,25] JNK is a stress-induced protein kinase and is involved in regulation of gene expression and stabilization through phosphorylation of Jun and other proteins.[26] Only the phosphorylated JNK (phospho-JNK), which is translocated to the nucleus, activates c-Jun.[27] The assembly of JNK and its upstream kinases (MAPKK and MAPKKK) requires molecular scaffold proteins, the JNK interacting proteins (JIPs).[28,29] Several studies have reported that JNK activity is increased in response to diabetes, and elevated JNK activity interferes with insulin action both in cell culture and in animal models.[30–33]

From the Departments of [1]Internal Medicine and [5]Physiology and the [6]JDRF Center for Complications in Diabetes, University of Michigan Medical School, Ann Arbor, Michigan; the [2]Department of Pharmaceutical Science, Toyama Medical and Pharmaceutical University, Toyama, Japan; the [3]Department of Molecular Biopharmacy and Genetics, Graduate School of Pharmaceutical Sciences, Tohoku University, Sendai, Japan; and the [4]Pennington Biomedical Research Center, Louisiana State University, Baton Rouge, Louisiana.

Supported by an ARVO/Novartis Research Fellowship Grant (JZ) and the JDRF Center for Complications in Diabetes (AKK) and in part by National Institutes of Health Grant RPO60DK-20572, which supports the Michigan Diabetes Research and Training Center.

Submitted for publication September 8, 2004; revised November 15, 2004, and March 22, 2005; accepted April 11, 2005.

Disclosure: **J. Zhou**, None; **B.K. Deo**, None; **K. Hosoya**, None; **T. Terasaki**, None; **I.G. Obrosova**, None; **F.C. Brosius, III**, None; **A.K. Kumagai**, None

The publication costs of this article were defrayed in part by page charge payment. This article must therefore be marked "*advertisement*" in accordance with 18 U.S.C. §1734 solely to indicate this fact.

Corresponding author: Arno K. Kumagai, Department of Internal Medicine, 5570 MSRB-2, Box 0678, Ann Arbor, MI 48109-0678; akumagai@umich.edu.

To understand whether increased intracellular glucose concentrations potentiate oxidative stress and activate the JNK signaling pathway in retinal endothelial cells, we established lines of stable transfected GLUT1-overexpressing rat retinal endothelial cells. In this report, we demonstrate that increased GLUT1 expression results in an increase in intracellular glucose and elevated oxidative stress and JNK phosphorylation in this cell line. These results indicate that the JNK signaling pathway is activated in response to increased glucose flux.

METHODS

Antibodies

The anti-phosphoJNK and anti-total JNK antibodies were from Santa Cruz Biotechnology, Inc. (Santa Cruz, CA); the anti-malondialdehyde (MDA) antibody from Abcam, Inc. (Cambridge, MA); and the anti-rabbit and anti-mouse antibodies coupled to horseradish peroxidase from GE Healthcare (Piscataway, NJ). Staining of transferred proteins on the Western blot membranes, as well as an anti-GAPDH monoclonal antibody (Advanced Immunochemical, Inc., Long Beach, CA) were used as internal loading controls. A polyclonal antibody raised against a purified human erythrocyte glucose transporter (GLUT1) was the kind gift of Christin Carter-Su (University of Michigan) and the polyclonal anti-JIP-1 antibodies were kindly provided by Benjamin Margolis (University of Michigan). The anti-GLUT1 and anti-JIP-1 antibodies have been characterized previously.[34,35]

Cell Culture

An immortalized rat retinal endothelial cell line TRiBRB, which was established from retinal capillaries isolated from transgenic rats carrying temperature-sensitive SV-40 large T antigen gene, was used in this study.[36] Although experiments investigating the endothelial cell biology of diabetic microvascular complications have frequently been performed in primary endothelial cell cultures of bovine or human origin, the well-known difficulty in transfecting retinal endothelial cells with exogenous DNA prevented use of a primary retinal endothelial cell culture model in these experiments.[37] The conditionally immortalized rat retinal endothelial cell line, TRiBRB, was therefore used to create stable retinal endothelial cell overexpression of GLUT1. TRiBRB cells are a well-described line that have typical characteristics of primary retinal endothelial cells in culture, including spindle-shaped morphology, expression of factor VIII, VEGF receptor-2, and p-glycoprotein, as well as uptake of acetylated LDL, and facilitated transport of glucose, oxidized vitamin C, and amino acids.[36,38–41] The cells were grown in DMEM (Invitrogen, Carlsbad, CA) supplemented with fetal bovine serum (10%), endothelial cell growth factor (15 μg/mL; Roche, Indianapolis, IN), heparin (100 μg/mL), and antibiotics and antimycotics (100 U/mL penicillin, 100 μg/mL streptomycin, and 250 ng/mL amphotericin B; Sigma-Aldrich, St. Louis, MO). To establish stable transfected cells, full-length human GLUT1 cDNA (a gift from Michael Mueckler, Washington University, St. Louis, MO) was subcloned into pcDNA3.1 at the *Bam*HI site (BD-Clontech, Palo Alto, CA) and transfected into TRiBRB cells. A pcDNA3.1 was also transfected into TRiBRB cells as a vector control. Stable transfected cells were propagated through G418 selection at 32°C. Cells were then switched to 37°C for all experiments. It has been shown that SV40 expression is substantially reduced after 1 to 2 days of culture at a nonpermissive temperature.[36] Expression of GLUT1 was determined by Western blot analysis.[42] All cells were collected at the same passages and same cell density.

Intracellular Glucose Measurement

Intracellular glucose concentration was measured by gas chromatography (GC)-mass spectrometry. Briefly, vector control and GLUT1-overexpressing cells were cultured in complete medium, as stated earlier including 5 mM glucose and allowed to grow to 90% confluence in six-well plates. Cells were then washed three times in cold 1× phosphate-buffered saline. After they were freeze-thawed three times, aliquots (200 μL) of supernatants were treated with trichloroacetic acid (final concentration 5% trichloroacetic acid [TCA]) and then derivatized with hydroxylamine and 4-dimethylamino pyridine.[43] A GC-mass spectrometer (5972 series; Hewlett Packard, Palo Alto, CA) was used to measure glucose concentrations. Aliquots were taken to determine total protein amount using bicinchoninic acid (BCA) protein assays, based on the manufacturer's instructions (Pierce Biotechnology, Inc., Rockford, IL). Intracellular glucose concentrations were compared between GLUT1-overexpressing and vector control cells.

Intracellular Reactive Oxygen Species Measurement

The intracellular reactive oxygen species was determined by a fluorescence detection method based on the oxidation of 5- (and -6)-chloromethyl-2′,7′- dichlorodihydrofluorescein diacetate, acetyl ester (CM-H_2DCFDA; Molecular Probes Inc., Eugene, OR).[8] GLUT1-overexpressing and vector control cells were grown in complete medium, as stated in the prior section, including 5 mM glucose, and allowed to grow in six-well plates until 90% confluence was achieved. CM-H_2DCFDA was added for 1 hour (20 μM) and fluorescence was analyzed by a cell sorter (Elite ESP; Beckman Coulter, Hialeah, FL) using excitation and emission wavelengths of 495 and 525 nm, respectively.

RNA Extraction, cDNA Microarray, and Northern Blot Analyses

GLUT1-overexpressing and vector control cells were grown in 5 mM glucose for 5 days to 90% confluence. Vector control and GLUT1-overexpressing cells were homogenized in extraction reagent (TRIzol; Invitrogen, Carlsbad, CA). Total RNA was extracted and further purified using an RNA cleanup procedure (RNeasy; Qiagen, Valencia, CA). RNA yields were assessed by absorbance at 260 nm, and the quality was confirmed on agarose-formaldehyde gels.

The cDNA microarray analysis was performed in conjunction with the Michigan NIDDK Biotechnology Core using a rat genome microarray (U34 chips; Affymetrix, Inc., Santa Clara, CA) containing gene expression data for >8000 known genes. Total RNA was extracted and purified as just described. Comparisons were made between GLUT1-overexpressing and vector control cells at normal glucose concentrations, to determine whether GLUT1 overexpression per se causes changes in gene expression profiles. Gene expression patterns detected by cDNA microarray analysis were confirmed in replicated experiments. Changes in gene expression that met a minimum of a twofold change, compared with control samples, were confirmed by Northern blot analysis.

To perform Northern blot analysis, total RNA was fractionated on agarose-formaldehyde gel electrophoresis. RNAs were transferred to membranes (Nytran SuPerCharge membrane; Schleicher & Schuell, Keene, NH) and hybridized with rat JIP-1b cDNA fragment and a housekeeping gene acidic ribosomal phosphoprotein PO (ARP/36B4) cDNA probe labeled with [α-^{32}P]dCTP by random primer labeling (GE Healthcare). The intensity of each band was visualized and quantified (PhosphorImager and Quantity One software; Bio-Rad, Hercules, CA).

Immunoblot and Immunoprecipitation

Vector control and GLUT1-overexpressing cells were washed three times in cold 1× phosphate-buffered saline and lysed in lysis buffer (1% SDS, 62.5 μM Tris [pH 6.8], 10% glycerol). As positive controls in MDA detection, both vector and GLUT1-overexpressing cells were treated with 80 μM H_2O_2 for 1 hour at 37°C. Cells were then rinsed twice with PBS. Proteins were resolved by electrophoresis on 10% SDS polyacrylamide gels, transferred to membranes (Hybond-P; GE Healthcare), and immuno-

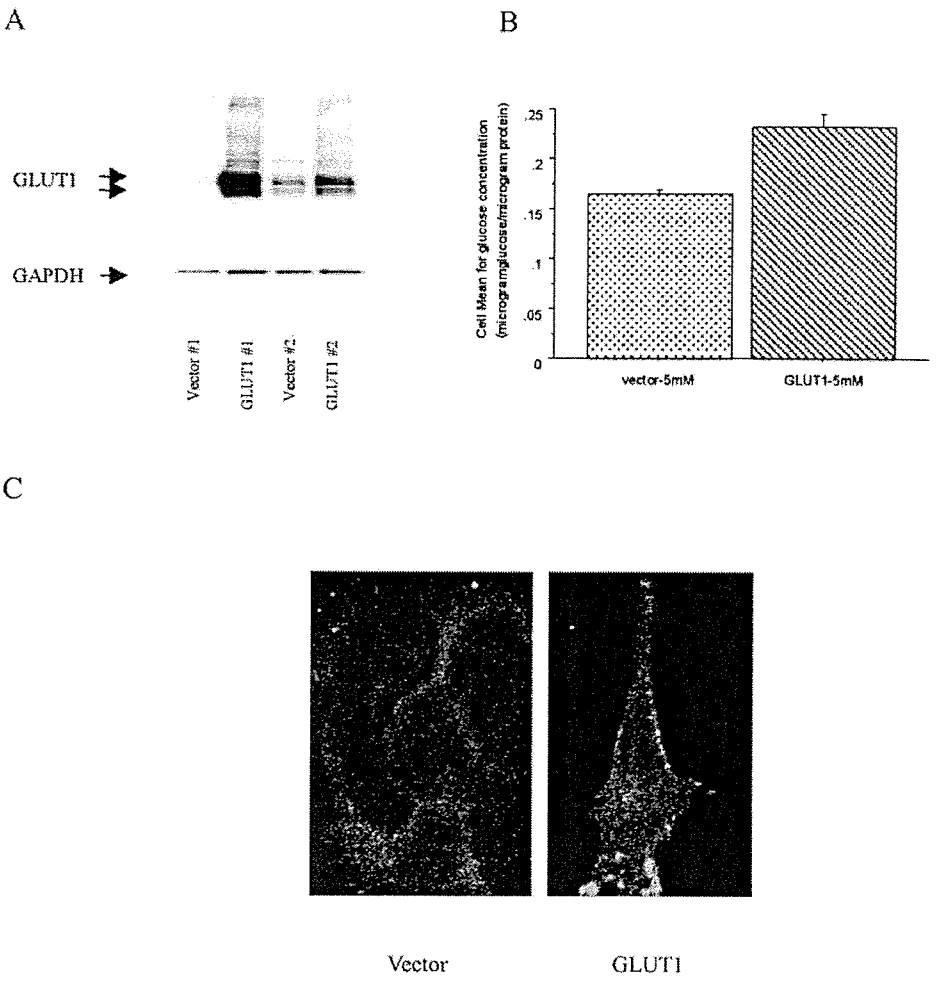

FIGURE 1. Vector control and GLUT-overexpressing cells[b]. (**A**) Western blot analysis for GLUT1 in vector and GLUT-overexpressing cells from two independent sets of clones (clone 1 and clone 2). Each lane contains 10 μg protein from whole-cell lysate. The membrane was first probed with anti-GLUT1 antibody, and then it was stripped and reprobed with anti-GAPDH antibody to serve as an internal loading control. (**B**) Intracellular glucose measurements in vector and GLUT1-overexpressing cells, by GC-mass spectrometry. Cells were cultured in medium containing 5 mM glucose. Data are the mean ± SE ($n = 6$). There was a statistically significant difference between the vector and GLUT1-overexpressing cells ($P = 0.0003$, Student's *t*-test). (**C**) Immunocytochemistry for GLUT1 in vector control and GLUT1-overexpressing cells. GLUT1 expression was detected by confocal microscopy. Magnification, ×600.

blotted with antibodies against GLUT1, total JNK, phosphoJNK, and MDA, followed by secondary horseradish peroxidase-anti-rabbit antibodies according to methods described previously.[42] Blots were visualized by a chemiluminescence assay (ECL-Plus; GE Healthcare, Piscataway, NJ). To verify equal loading of proteins, Western blots were stained with ponceau-S after transfer. In addition, after immunoblot, each blot was stripped and reprobed with an anti-GAPDH antibody, as an internal control.

To perform immunoprecipitation, vector control and GLUT1-overexpressing cells were washed in 1× phosphate-buffered saline and scraped with a cell scraper in lysis buffer (50 mM HEPES [pH 7.5], 10% glycerol, 150 mM NaCl, 1% Triton X-100, 1.5 mM $MgCl_2$,1 mM EGTA, 1 mM phenylmethylsulfonyl fluoride, 100 mM NaF, 200 mM sodium orthovanadate, 10 mM tetrasodium pyrophosphate, 10 mg aprotinin/mL and 10 mg leupeptin/mL).[35] Lysates (4.5 mg) were incubated with a anti-JIP-1 antibody (antiserum no. 152) and protein A agarose (RepliGen Corp., Waltham, MA) overnight at 4°C. Pellets were washed three times in washing buffer (20 mM HEPES [pH 7.5], 150 mM NaCl, 10% glycerol, and 0.1% Triton X-100) and boiled in 1× sample buffer. Supernatants were resolved by 8% SDS polyacrylamide gel electrophoresis, transferred to a membrane (Hybond-P; GE Healthcare), and immunoblotted with antibodies against JIP-1, GLUT1, total JNK, and phosphoJNK. Blots were visualized by chemiluminescence as above (ECL Plus; GE Healthcare).

Immunohistochemistry

Vector control and GLUT1-overexpressing cells were grown on chamber slides to 90% confluence. Cells were fixed with 4% paraformaldehyde for 30 minutes at room temperature and permeabilized with 0.1% Triton X-100 in 1× phosphate-buffered saline for 10 minutes. The slides were blocked with 1% goat serum for 1 hour and incubated with either anti-GLUT1 (1:500 dilution) or anti-JIP-1 (1:250 dilution) overnight. After washing, the slides were incubated with goat anti-rabbit-FITC (1:200 dilution; Molecular Probes) for 1 hour, and mounted (Prolong; Molecular Probes) and viewed with a laser scanning confocal microscope (model OZ; Noran Instruments, Middleton, WI).

Statistical Analysis

Comparisons between vector control and GLUT1-overexpressing cells were made with Student's *t*-test. $P < 0.05$ was considered significant.

RESULTS

Increased Glucose Flux in GLUT1-Overexpressing Cells

Under normal culture conditions, immortalized rat retinal endothelial cells overexpressing GLUT1 showed an approximate four- to eightfold increase in GLUT1 expression compared with vector control cells (Fig. 1A). Such levels of expression were confirmed by Western blot in every experiment performed. Increased GLUT1 expression resulted in increased intracellular glucose, as determined by GC-mass spectrometry (Fig. 1B). There was an average 40% increase in intracellular glucose in GLUT1-overexpressing cells compared with vector control

cells, and the increase was statistically significant ($P = 0.0003$; Fig. 1B). Immunohistochemistry confirmed membrane expression of GLUT1 protein in both vector control and GLUT1-overexpressing cells (Fig 1C). Increased GLUT1 expression was also visible in GLUT1-overexpressing cells, with much of GLUT1 protein localized in the cytoplasmic membrane.

Increased Oxidative Stress in GLUT1-Overexpressing Cells

The presence of free glucose in the retinal endothelial cells may provide a substrate for a variety of biochemical processes. We examined the possibility that GLUT1-overexpression induces oxidative stress in TRiBRB cells. GLUT1-overexpressing and vector control cells were incubated with CM-H_2DCFDA (20 μM) for 1 hour, and the fluorescence was measured by flow cytometry (FACScan; BD Biosciences, Franklin Lakes, NJ). As shown in Figure 2A, there was approximately an 80% increase in generation of DCF-sensitive ROS in GLUT1-overexpressing compared with vector control cells, a statistically significant increase ($P < 0.0001$). To determine whether lipid peroxidation products were increased with GLUT1-overexpression, GLUT1-overexpressing and vector control cells were grown in 5 mM glucose, and Western blot analysis was performed using antibody against MDA-protein addicts. Identical cultures were treated with 80 μM H_2O_2 for 1 hour as positive controls. As shown in Figure 2B, there was increased lipid peroxidation in GLUT1-overexpressing cells as determined by increased MDA-modified protein addicts in Western blot analysis (Fig. 2B). The most prominent MDA-modified protein adducts were of higher molecular weight, approximately 200 and 80 kDa, in GLUT1-overexpressing cells compared to vector control cells.

Increased JNK Phosphorylation in GLUT1-Overexpressing Cells

Increased JNK activity in response to high glucose has been reported in human umbilical vein endothelial cells.[44] To assess whether increased glucose flux through increased GLUT1 expression also results in the phosphorylation of JNK in retinal endothelial cells, we performed Western blot analysis and probed the blots with anti-phosphoJNK and total JNK. As shown in Figure 3, there was a basal level of JNK phosphorylation in vector control cells. Increased GLUT1 expression and increased glucose flux resulted in an increase in JNK phosphorylation. There was no detectable change in total JNK (Fig. 3). Western blot with an anti-p38 antibody revealed no change in p38 protein expression (data not shown).

Increased JIP-1 Expression in GLUT1-Overexpressing Cells

To identify additional molecular changes in GLUT1-overexpressing cells, cDNA microarray analysis was performed using a rat genome microarray (Set U34; Affymetrix, Inc.). We found increased JIP-1 gene expression among the upregulated genes. JIP-1 expression was increased more than twofold in two replicates (Fig. 4A). To confirm the observed changes in JIP-1 expression, we performed Northern blot analysis. As shown in Figure 4B, there was an approximate 80% increase in JIP-1 expression in GLUT1-overexpressing cells compared with that in vector control cells. The expression of transcripts of enzymes involved in glycolytic, polyol, and hexosamine pathways were unchanged in the overexpressing cells compared with the vector control (data not shown).

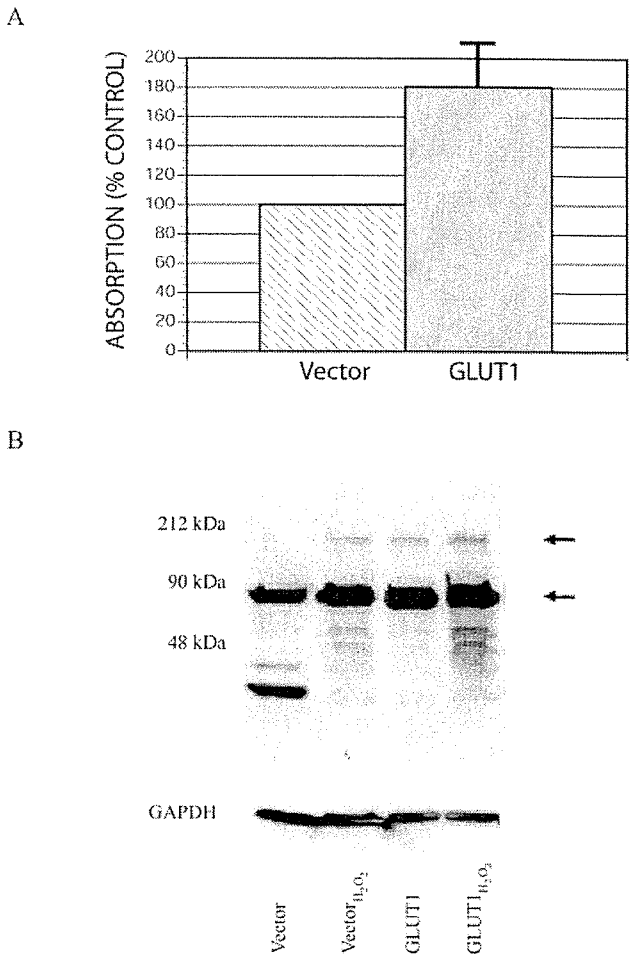

FIGURE 2. Oxidative stress measurements in vector and GLUT1-overexpressing cells. (A) DCF measurement in vector and GLUT1-overexpressing cells. Cells were grown in complete medium containing 5 mM glucose and allowed to grow in six-well plates until 90% confluence was achieved. CM-H_2DCFDA was added for 1 hour (20 μM) and analyzed by flow cytometry, using excitation and emission wavelengths of 495 and 525 nm, respectively. (B) Western blot for MDA-modified protein adducts in vector and GLUT1-overexpressing cells. Each lane contains 30 μg protein from whole-cell lysate. Vector control and GLUT1-overexpressing cells treated with 80 μM H_2O_2 were used as a positive control for detecting MDA-modified protein adducts. After probing with anti-MDA antibody, the membrane was stripped and reprobed with GAPDH as the loading control.

Association of JIP-1 with PhosphoJNK

Endogenous JIP-1 protein has been detected mainly in pancreatic islet and neuronal cells.[35,45] To determine whether JIP-1 protein is expressed in retinal endothelial cells, we performed immunoprecipitation using whole-cell lysates (4.5 mg).[35] In both vector control and GLUT1-overexpressing cells, a prominent band corresponding to 90 kDa was detected by antibodies against both JIP-1 carboxyl-terminal peptide (antiserum no. 176) and GST-JIP-1 Src homology 3 domain fusion protein (antiserum no. 152),[35] which was consistent with JIP-1 detected in neuronal cells (Fig. 5A).[35,45] As a JNK scaffold protein, JIP-1 binds to three kinases, MLK3, MAP2K7, and JNK, to form a signaling complex.[28,46] In both vector control and GLUT1-overexpressing cells, phosphorylated JNK was found to coimmunoprecipitate with JIP-1 (Fig. 5B), which is consistent

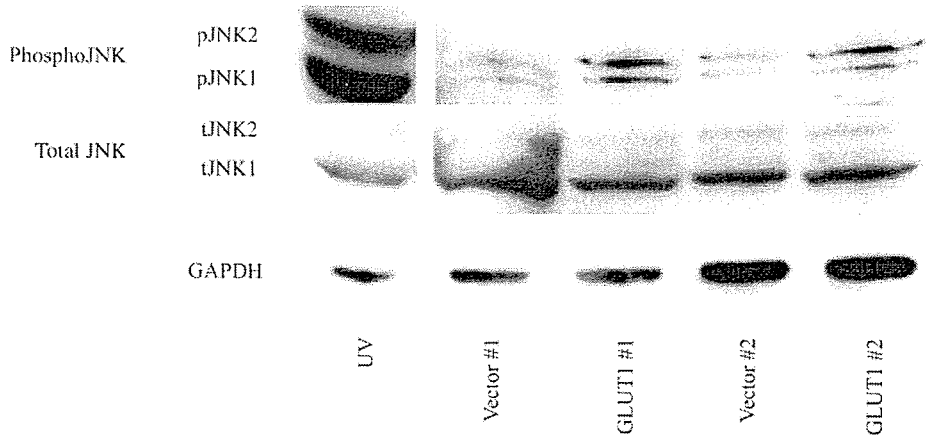

FIGURE 3. Western blot of phosphorylated JNK and total JNK in vector control and GLUT1-overexpressing cells. Vector control and GLUT1-overexpressing cells from two independent clone sets were cultured in medium containing 5 mM glucose. Each lane contains 20 μg protein from whole-cell lysate, except for the UV control lane (5 μg/lane). Human embryonic kidney 293 cells were treated with 400 μJ of UV light to induce JNK phosphorylation and served as positive control for phosphorylated JNK. The membrane was first probed with anti-phosphorylated JNK. The membrane was then stripped and reprobed with anti-total JNK antibody. After the second stripping, the membrane was probed with anti-GAPDH antibody, as an internal loading control.

A

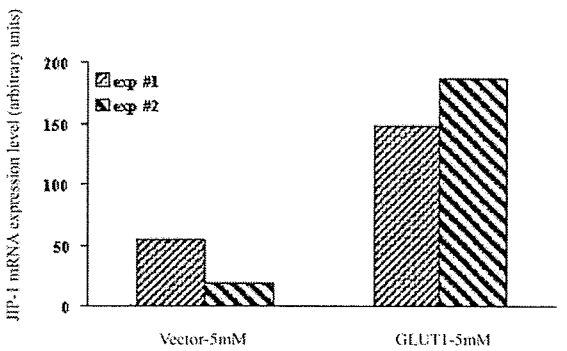

B

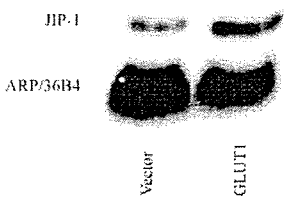

FIGURE 4. Upregulation of the JIP-1 gene in GLUT1-overexpressing cells compared with vector control cells, detected by cDNA microarray analysis (**A**). GLUT1-overexpressing and vector control cells were cultured in medium containing 5 mM glucose for 5 days. Results are from two independent cDNA microarray analyses. JIP-1 was upregulated by more than twofold in both experiments. (**B**) Northern blot of JIP-1 in vector control and GLUT1-overexpressing cells. Total RNA was extracted from vector control and GLUT1-overexpressing cells. Each lane contained 25 μg total RNA. The membrane was probed with a ^{32}P-labeled JIP-1 fragment and ARP/36B4.

with the role of JIP-1 as a scaffold protein essential in JNK activation. Immunoprecipitation also showed a basal level of JNK phosphorylation associated with JIP-1 in vector control cells. JIP-1 has been reported to be in direct contact with cell surface receptors, guanine exchange factor, and motor kinesin,[35,47–49] however, GLUT1 did not coimmunoprecipitate with JIP-1 (data not shown).

Subcellular Localization of JIP-1 in Retinal Endothelial Cells

To determine the localization of endogenous JIP-1 in retinal endothelial cells, both vector control and GLUT1-overexpressing cells were stained by indirect immunofluorescence. JIP-1 was found to be predominantly localized in the cytoplasm, especially in the perinuclear area. Confocal microscopy revealed that a small amount of JIP-1 was localized in the nucleus (Fig. 6). The pattern of JIP-1 staining was similar in both vector control and GLUT1-overexpressing cells.

DISCUSSION

In this study, we report changes in oxidative stress and JNK phosphorylation in stable transfected GLUT1-overexpressing rat retinal endothelial cells in response to increased intracellular glucose. Our results demonstrate that increased oxidative stress and JNK phosphorylation resulted from increased glucose flux through increased GLUT1 expression. The increased JNK phosphorylation probably occurs through upregulation of JIP-1, as evidenced by physical association of JIP-1 with phosphorylated JNK protein.

Increased glucose has been shown to generate increased reactive oxygen species (ROS) in cell types susceptible to hyperglycemic damage, such as endothelial cells and mesangial cells.[50,51] In our study, we found an approximate 80% increase in generation of cytosolic ROS, which was detected by DCF in GLUT1-overexpressing compared with vector control cells. It has been suggested that high-glucose–induced ROS production mainly consists of hydrogen peroxide.[51] In mesangial cells, H_2O_2 was produced through increased glucose uptake and glucose metabolism rather than glucose auto-oxidation and can

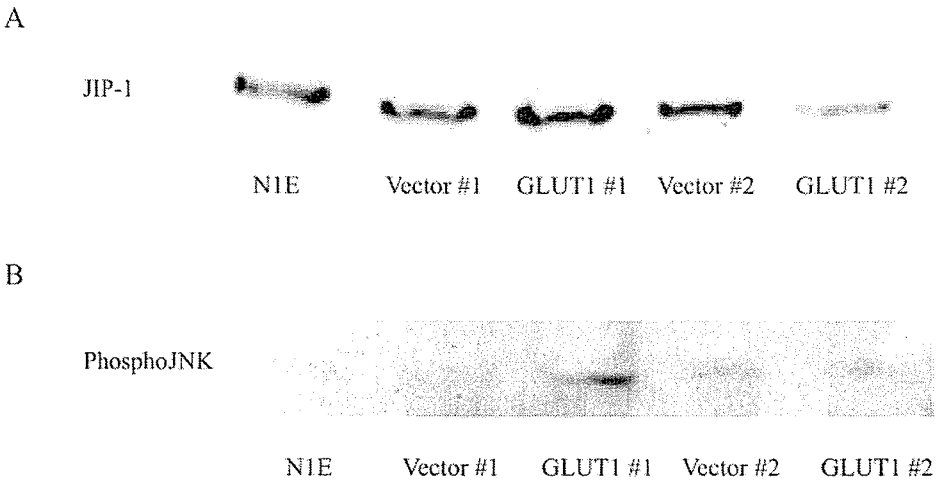

FIGURE 5. Coimmunoprecipitation of JIP-1 and phosphorylated JNK in both vector and GLUT1-overexpressing cells. (A) Lysates from vector and GLUT1-overexpressing cells were immunoprecipitated with anti-JIP-1 antibody (antiserum no. 152) and immunoblotted with anti-JIP-1 (antiserum no. 176). Mouse neuroblastoma N1E-115 cells were used as a positive control for JIP-1. Two sets of independent clones were used in the experiments (marked #1 and #2). (B) After probing with anti-JIP-1 antibody (antiserum no. 176), the membrane was stripped and reprobed with anti-phosphorylated JNK antibody to detect the presence of phosphorylated JNK.

be effectively inhibited by catalase.[51] Although the ROS species generated in retinal endothelial cells remains to be determined, our initial experiments did not find significant changes in catalase activity. Our study also detected increased MDA-modified protein addicts at higher molecular weight (approximately 80 and 200 kDa), which suggested increased lipid peroxidation—a marker of oxidative stress-in GLUT1-overexpressing cells. Previous studies in diabetic subjects have shown that lipid peroxidation in both plasma and the vitreous body is linked to the development and progression of diabetic retinopathy. The reduction of lipid peroxidation in patients with rigorously controlled diabetes conferred a 50% lower risk of development of proliferative retinal changes, compared with standard glucose control subjects.[52]

Recent studies found that the JNK pathway plays an important role in the development and progression of diabetes and its complications.[30-33,44,53-55] Increased ambient glucose results in growth retardation in several primary endothelial cell cultures, such as human umbilical vein endothelial cells (HUVECs), bovine pulmonary artery endothelial cells (PAECs), and cultured human endothelial cells.[56-58] The inhibition of cell growth has been suggested to be associated with JNK activation.[53] JNK activation induced by increased glucose was detected both in neurons and endothelial cells.[53,54] Our data also showed increased JNK phosphorylation to be associated with increased glucose flux and GLUT1 overexpression in rat retinal endothelial cells.

The identification of JIP-1 upregulation and increased JNK phosphorylation in the present study suggests that JIP-1 potentiates JNK activation in response to increased glucose flux through GLUT1 overexpression. This raises intriguing questions regarding the molecular events that connect increased glucose flux and increased JNK activity. JIP-1/IB1 has been reported as a nuclear protein that binds to the GLUT2 promoter and regulates GLUT2 expression in islet cells.[45] In neurons, JIP-1 is located in cytoplasm. On neuronal differentiation, JIP-1 concentrates at the extending end of neurites.[35] In our study, JIP-1 was mainly localized in the cytoplasm, especially the perinuclear area. JIP-1 has been shown to interact with several membrane receptors to form a signaling complex.[47,48,59] JIP-1 has also been detected to interact with an exchange factor for the small GTPase RhoA and molecular motor kinesin to regulate cytoskeleton rearrangement in neuronal cells.[35,49] Our study did not find a physical association between JIP-1 and GLUT1.

Increased oxidative stress has been linked to the activation of JNK pathway in many cell types.[60,61] Hydrogen peroxide produced during oxidative stress has been shown to be a potent activator that induces JNK activation in skeletal muscle fibers.[60] Studies in bovine lung microvascular endothelial cells have indicated that increased glutathione reductase activity inhibits JNK activation.[61] Although we did not determine whether increased lipid peroxidation is directly linked to increased JNK phosphorylation in the present study, given the above experimental observations conducted in other cell types, we speculate that there is a mechanistic link between increased lipid peroxidation and JNK phosphorylation in response to increased glucose flux through increased GLUT1 expression in rat retinal endothelial cells. The pathologic consequences associated with increased oxidative stress and JNK

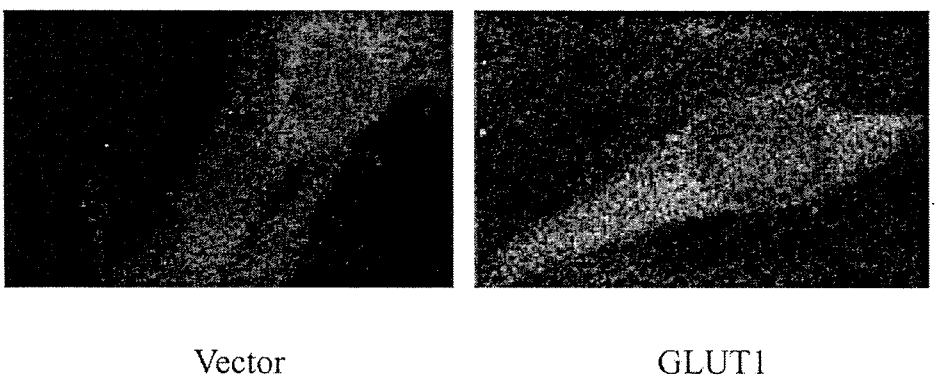

FIGURE 6. Immunocytochemistry for JIP-1 in vector control and GLUT1-overexpressing cells grown on chambered slides. JIP-1 protein was detected with anti-JIP-1 antibody (antiserum no. 152). JIP-1 expression was visualized by confocal microscopy. Magnification, ×600.

phosphorylation in retinal endothelial cells remain to be determined.

Acknowledgments

The authors thank Kelli Sullivan, Stephen Lentz, and the staff of the JDRF Morphology Core for assistance with morphologic analysis and Martin J. Stevens and Judy Grossi for help with the GC-Mass spectrometry measurements.

References

1. Robison WG, Kinoshita JH, Kador PF. The polyol pathway in retinal microangiopathy. *Drugs*. 1986;32:19-22.
2. Heath H, Paterson RA, Hart JC. Changes in the hydroxyproline, hexosamine and sialic acid of the diabetic human and beta, beta'-iminodipropionitrile-treated rat retinal vascular systems. *Diabetologia*. 1967;3:515-518.
3. Nakamura M, Barber AJ, Antonetti DA, et al. Excessive hexosamines block the neuroprotective effect of insulin and induce apoptosis in retinal neurons. *J Biol Chem*. 2001;276:43748-43755.
4. Stitt AW, Jenkins AJ, Cooper ME. Advanced glycation end products and diabetic complications. *Expert Opin Investig Drugs*. 2002;11:1205-1223.
5. Stitt AW, Li YM, Gardiner TA, Bucala R, Archer DB, Vlassara H. Advanced glycation end products (AGEs) co-localize with AGE receptors in the retinal vasculature of diabetic and of AGE-infused rats. *Am J Pathol*. 1997;150:523-531.
6. King GL, Kunisaki M, Nishio Y, Inoguchi T, Shiba T, Xia P. Biochemical and molecular mechanisms in the development of diabetic vascular complications. *Diabetes*. 1996;45:S105-S108.
7. Lorenzi M, Montisano DF, Toledo S, Barrieux A. High glucose induces DNA damage in cultured human endothelial cells. *J Clin Invest*. 1986;77:322-325.
8. Nishikawa T, Edelstein D, Du XL, et al. Normalizing mitochondrial superoxide production blocks three pathways of hyperglycaemic damage. *Nature*. 2000;404:787-790.
9. Klein R, Klein BE, Moss SE, Davis MD, DeMets DL. The Wisconsin epidemiologic study of diabetic retinopathy. III. Prevalence and risk of diabetic retinopathy when age at diagnosis is 30 or more years. *Arch Ophthalmol*. 1984;102:527-532.
10. Klein R, Klein BE, Moss SE, Davis MD, DeMets DL. The Wisconsin epidemiologic study of diabetic retinopathy. II. Prevalence and risk of diabetic retinopathy when age at diagnosis is less than 30 years. *Arch Ophthalmol*. 1984;102:520-526.
11. The Diabetes Control, Complications Trial Research Group. The effect of intensive treatment of diabetes on the development and progression of long-term complications in insulin-dependent diabetes mellitus. *N Engl J Med*. 1993;329:977-986.
12. UKPDS. Intensive blood-glucose control with sulphonylureas or insulin compared with conventional treatment and risk of complications in patients with type 2 diabetes (UKPDS 33). UK Prospective Diabetes Study (UKPDS) Group. *Lancet*. 1998;352:837-853.
13. Cogan D, Toussaint D, Kuwabara T. Retinal vascular patterns. IV. Diabetic retinopathy. *Arch Ophthalmol*. 1961;66:366-378.
14. Kumagai AK, Glasgow BJ, Pardridge WM. GLUT1 glucose transporter expression in the diabetic and nondiabetic human eye. *Invest Ophthalmol Vis Sci*. 1994;35:2887-2894.
15. Harik SI, Kalaria RN, Whitney PM, et al. Glucose transporters are abundant in cells with "occluding" junctions at the blood-eye barriers. *Proc Natl Acad Sci U S A*. 1990;87:4261-4264.
16. Takata K, Hirano H, Kasahara M. Transport of glucose across the blood-tissue barriers. *Int Rev Cytol*. 1997;172:1-53.
17. Berkowitz BA, Garner MH, Wilson CA, Corbett RJ. Nondestructive measurement of retinal glucose transport and consumption in vivo using NMR spectroscopy. *J Neurochem*. 1995;64:2325-2331.
18. Olgemoller B, Schleicher ED, Gerbitz KD. Differential kinetics of glucose metabolism in porcine retinal and aortic endothelial cells. *J Clin Chem Clin Biochem*. 1990;28:15-17.
19. Schmidt AM, Hori O, Cao R, et al. RAGE: a novel cellular receptor for advanced glycation end products. *Diabetes*. 1996;45:S77-S80.
20. Lander HM, Tauras JM, Ogiste JS, Hori O, Moss RA, Schmidt AM. Activation of the receptor for advanced glycation end products triggers a p21(ras)-dependent mitogen-activated protein kinase pathway regulated by oxidant stress. *J Biol Chem*. 1997;272:17810-17814.
21. Yan SD, Schmidt AM, Anderson GM, et al. Enhanced cellular oxidant stress by the interaction of advanced glycation end products with their receptors/binding proteins. *J Biol Chem*. 1994;269:9889-9897.
22. Min C, Kang E, Yu SH, Shinn SH, Kim YS. Advanced glycation end products induce apoptosis and procoagulant activity in cultured human umbilical vein endothelial cells. *Diabetes Res Clin Pract*. 1999;46:197-202.
23. Yamagishi S, Inagaki Y, Okamoto T, et al. Advanced glycation end product-induced apoptosis and overexpression of vascular endothelial growth factor and monocyte chemoattractant protein-1 in human-cultured mesangial cells. *J Biol Chem*. 2002;277:20309-20315.
24. Kawamori D, Kajimoto Y, Kaneto H, et al. Oxidative stress induces nucleo-cytoplasmic translocation of pancreatic transcription factor PDX-1 through activation of c-Jun NH(2)-terminal kinase. *Diabetes*. 2003;52:2896-2904.
25. Zhang L, Zalewski A, Liu Y, et al. Diabetes-induced oxidative stress and low-grade inflammation in porcine coronary arteries. *Circulation*. 2003;108:472-478.
26. Kallunki T, Deng T, Hibi M, Karin M. c-Jun can recruit JNK to phosphorylate dimerization partners via specific docking interactions. *Cell*. 1996;87:929-939.
27. Gupta S, Campbell D, Derijard B, Davis RJ. Transcription factor ATF2 regulation by the JNK signal transduction pathway. *Science*. 1995;267:389-393.
28. Whitmarsh AJ, Cavanagh J, Tournier C, Yasuda J, Davis RJ. A mammalian scaffold complex that selectively mediates MAP kinase activation. *Science*. 1998;281:1671-1674.
29. Dickens M, Rogers JS, Cavanagh J, et al. A cytoplasmic inhibitor of the JNK signal transduction pathway. *Science*. 1997;277:693-696.
30. Carlson CJ, Koterski S, Sciotti RJ, Poccard GB, Rondinone CM. Enhanced basal activation of mitogen-activated protein kinases in adipocytes from type 2 diabetes: potential role of p38 in the downregulation of GLUT4 expression. *Diabetes*. 2003;52:634-641.
31. Hirosumi J, Tuncman G, Chang L, et al. A central role for JNK in obesity and insulin resistance. *Nature*. 2002;420:333-336.
32. Fujishiro M, Gotoh Y, Katagiri H, et al. Three mitogen-activated protein kinases inhibit insulin signaling by different mechanisms in 3T3-L1 adipocytes. *Mol Endocrinol*. 2003;17:487-497.
33. Fernyhough P, Gallagher A, Averill SA, et al. Aberrant neurofilament phosphorylation in sensory neurons of rats with diabetic neuropathy. *Diabetes*. 1999;48:881-889.
34. Tai PK, Liao JF, Chen EH, Dietz J, Schwartz J, Carter-Su C. Differential regulation of two glucose transporters by chronic growth hormone treatment of cultured 3T3-F442A adipose cells. *J Biol Chem*. 1990;265:21828-21834.
35. Meyer D, Liu A, Margolis B. Interaction of c-Jun amino-terminal kinase interacting protein-1 with p190 rhoGEF and its localization in differentiated neurons. *J Biol Chem*. 1999;274:35113-35118.
36. Hosoya K, Tomi M, Ohtsuki S, et al. Conditionally immortalized retinal capillary endothelial cell lines (TR-iBRB) expressing differentiated endothelial cell functions derived from a transgenic rat. *Exp Eye Res*. 2001;72:163-172.
37. Tanner FC, Carr DP, Nabel GJ, Nabel EG. Transfection of human endothelial cells. *Cardiovasc Res*. 1997;35:522-528.
38. Tomi M, Hosoya K, Takanaga H, Ohtsuki S, Terasaki T. Induction of xCT gene expression and L-cystine transport activity by diethyl maleate at the inner blood-retinal barrier. *Invest Ophthalmol Vis Sci*. 2002;43:774-779.
39. Hosoya K, Kondo T, Tomi M, Takanaga H, Ohtsuki S, Terasaki T. MCT1-mediated transport of L-lactic acid at the inner blood-retinal barrier: a possible for delivery of monocarboxylic acid drugs to the retina. *Pharm Res*. 2001;18:1669-1676.

40. Hosoya K, Minamizono A, Katayama K, Terasaki T, Tomi M. Vitamin C transport in oxidized form across the rat blood-retinal barrier. *Invest Ophthalmol Vis Sci.* 2004;45:1232–1239.
41. Hosoya K, Saeki S, Terasaki T. Activation of carrier-mediated transport of L-cystine at the blood-brain and blood-retinal barriers in vivo. *Microvasc Res.* 2001;62:136–142.
42. Sone H, Deo BK, Kumagai AK. Enhancement of glucose transport by vascular endothelial growth factor in retinal endothelial cells. *Invest Ophthalmol Vis Sci.* 2000;41:1876–1884.
43. Guerrant G, Moss C. Determination of monosaccharides as aldononitrile, O-methyloxime, alditol, and cyclitol acetate derivatives by gas chromatography. *Anal Chem.* 1984;56:633–638.
44. Ho FM, Liu SH, Liau CS, Huang PJ, Lin-Shiau SY. High glucose-induced apoptosis in human endothelial cells is mediated by sequential activations of c-Jun NH(2)-terminal kinase and caspase-3. *Circulation.* 2000;101:2618–2624.
45. Bonny C, Nicod P, Waeber G. IB1, a JIP-1-related nuclear protein present in insulin-secreting cells. *J Biol Chem.* 1998;273:1843–1846.
46. Yasuda J, Whitmarsh AJ, Cavanagh J, Sharma M, Davis RJ. The JIP group of mitogen-activated protein kinase scaffold proteins. *Mol Cell Biol.* 1999;19:7245–7254.
47. Matsuda S, Yasukawa T, Homma Y, et al. c-Jun N-terminal kinase (JNK)-interacting protein-1b/islet-brain-1 scaffolds Alzheimer's amyloid precursor protein with JNK. *J Neurosci.* 2001;21:6597–6607.
48. Gotthardt M, Trommsdorff M, Nevitt MF, et al. Interactions of the low density lipoprotein receptor gene family with cytosolic adaptor and scaffold proteins suggest diverse biological functions in cellular communication and signal transduction. *J Biol Chem.* 2000;275:25616–25624.
49. Verhey KJ, Meyer D, Deehan R, et al. Cargo of kinesin identified as JIP scaffolding proteins and associated signaling molecules [comment]. *J Cell Biol.* 2001;152:959–970.
50. Pieper GM, Langenstroer P, Siebeneich W. Diabetic-induced endothelial dysfunction in rat aorta: role of hydroxyl radicals. *Cardiovasc Res.* 1997;34:145–156.
51. Ha H, Lee HB. Reactive oxygen species as glucose signaling molecules in mesangial cells cultured under high glucose. *Kidney Int Suppl.* 2000;77:S19–S25.
52. Augustin AJ, Dick HB, Koch F, Schmidt-Erfurth U. Correlation of blood-glucose control with oxidative metabolites in plasma and vitreous body of diabetic patients. *Eur J Ophthalmol.* 2002;12:94–101.
53. Liu W, Schoenkerman A, Lowe WL Jr. Activation of members of the mitogen-activated protein kinase family by glucose in endothelial cells. *Am J Physiol.* 2000;279:E782–E790.
54. Purves T, Middlemas A, Agthong S, et al. A role for mitogen-activated protein kinases in the etiology of diabetic neuropathy. *FASEB J.* 2001;15:2508–2514.
55. Waeber G, Delplanque J, Bonny C, et al. The gene MAPK8IP1, encoding islet-brain-1, is a candidate for type 2 diabetes. *Nat Genet.* 2000;24:291–295.
56. Curcio F, Ceriello A. Decreased cultured endothelial cell proliferation in high glucose medium is reversed by antioxidants: new insights on the pathophysiological mechanisms of diabetic vascular complications. *In Vitro Cell Dev Biol.* 1992;28A:787–790.
57. Morishita R, Aoki M, Nakamura S, et al. Potential role of a novel vascular modulator, hepatocyte growth factor (HGF), in cardiovascular disease: characterization and regulation of local HGF system. *J Atheroscler Thromb.* 1997;4:12–19.
58. Lorenzi M, Nordberg JA, Toledo S. High glucose prolongs cell-cycle traversal of cultured human endothelial cells. *Diabetes.* 1987;36:1261–1267.
59. Stockinger W, Brandes C, Fasching D, et al. The reelin receptor ApoER2 recruits JNK-interacting proteins-1 and -2. *J Biol Chem.* 2000;275:25625–25632.
60. Filosto M, Tonin P, Vattemi G, Savio C, Rizzuto N, Tomelleri G. Transcription factors c-Jun/activator protein-1 and nuclear factor-kappa B in oxidative stress response in mitochondrial diseases. *Neuropathol Appl Neurobiol.* 2003;29:52–59.
61. Hojo Y, Saito Y, Tanimoto T, et al. Fluid shear stress attenuates hydrogen peroxide-induced c-Jun NH2-terminal kinase activation via a glutathione reductase-mediated mechanism. *Circ Res.* 2002; 91:712–718.

L-Type Amino Acid Transporter 1–Mediated L-Leucine Transport at the Inner Blood–Retinal Barrier

Masatoshi Tomi,[1] *Masahiko Mori,*[1] *Masanori Tachikawa,*[2,3] *Kazunori Katayama,*[1] *Tetsuya Terasaki,*[2,4,5] *and Ken-ichi Hosoya*[1]

Purpose. L-type amino acid transporters (LATs) prefer branched-chain and aromatic amino acids, including neurotransmitter precursors. The objective of this study was to clarify the expression and function of LAT at the inner blood–retinal barrier (BRB).

Methods. [^{3}H]L-Leucine transport at the inner BRB was characterized by using in vivo integration plot analysis and a conditionally immortalized rat retinal capillary endothelial cell line (TR-iBRB2). The expression of the LAT1 was demonstrated by quantitative real-time RT-PCR, immunoblot, and immunohistochemical analyses.

Results. The apparent influx permeability clearance of [^{3}H]L-leucine in the rat retina was found to be 203 μL/(min · g retina), supporting a carrier-mediated influx transport of L-leucine at the BRB. [^{3}H]L-Leucine uptake by TR-iBRB2 cells was an Na^+-independent and concentration-dependent process with a K_m of 14.1 μM. This process was more potently *cis* inhibited by substrates of LAT1, D-leucine, D-phenylalanine, and D-methionine, than those of LAT2, L-alanine, and L-glutamine. [^{3}H]L-Leucine efflux from TR-iBRB2 cells was *trans*-stimulated by substrates of LAT1. The expression of LAT1 mRNA was 100- and 15-fold greater than that of LAT2 in TR-iBRB2 and magnetically isolated rat retinal vascular endothelial cells, respectively. The expression of LAT1 protein was observed in TR-iBRB2 and primary cultured human retinal endothelial cells and immunostaining of LAT1 was observed along the rat retinal capillaries.

Conclusions. LAT1 is expressed at the inner BRB and mediates blood-to-retina L-leucine transport. This transport system plays a key role in maintaining large neutral amino acids as well as neurotransmitters in the neural retina. (*Invest Ophthalmol Vis Sci.* 2005;46:2522–2530) DOI:10.1167/iovs.04-1175

From the [1]Faculty of Pharmaceutical Sciences, Toyama Medical and Pharmaceutical University, Toyama, Japan; the [2]Department of Molecular Biopharmacy and Genetics, Graduate School of Pharmaceutical Sciences, and the [4]New Industry Creation Hatchery Center, Tohoku University, Sendai, Japan; and [5]Solution Oriented Research for Science and Technology of the Japan Science and Technology Agency (JST), Kawaguchi, Japan.

[3]Present affiliation: Faculty of Pharmaceutical Sciences, Toyama Medical and Pharmaceutical University, Toyama, Japan.

Supported, in part, by a Grant-in-Aid for Scientific Research from the Japan Society for the Promotion of Science and a grant for Research on Sensory and Communicative Disorders by the Ministry of Health, Labor, and Welfare, Japan.

Submitted for publication October 5, 2004; revised February 25, 2005; accepted March 22, 2005.

Disclosure: **M. Tomi**, None; **M. Mori**, None; **M. Tachikawa**, None; **K. Katayama**, None; **T. Terasaki**, None; **K. Hosoya**, None

The publication costs of this article were defrayed in part by page charge payment. This article must therefore be marked "*advertisement*" in accordance with 18 U.S.C. §1734 solely to indicate this fact.

Corresponding author: Ken-ichi Hosoya, Faculty of Pharmaceutical Sciences, Toyama Medical and Pharmaceutical University, 2630, Sugitani, Toyama, 930-0194, Japan; hosoyak@ms.toyama-mpu.ac.jp.

L-Glutamate and its metabolic product, γ-aminobutyric acid (GABA) are the main neurotransmitters in the retina. The retinal L-glutamate pool is exclusively derived from de novo L-glutamate synthesis in the retina, since there is virtually no uptake of plasma L-glutamate into the retina.[1] Therefore, the retina requires branched-chain amino acids (leucine, isoleucine, and valine), particularly leucine, and glucose as, respectively, the main nitrogen and carbon precursors of retinal L-glutamate synthesis.[2,3] Branched-chain amino acids also serve as a source of carbon skeletons for the tricarboxylic acid cycle, and a substrate of protein synthesis, since branched-chain amino acids are essential amino acids. The nutrient supply to the retina from the circulating blood is regulated by the blood–retinal barrier (BRB), which is composed of retinal capillary endothelial cells (inner BRB) and retinal pigment epithelial cells (RPE, outer BRB).[4,5] It is well established that glucose is supplied from the circulating blood to the retina via GLUT1 at the BRB,[6,7] and this evidence prompted the hypothesis that the BRB has a supply system(s) to provide the branched-chain amino acids to maintain retinal concentrations of L-glutamate and GABA as well as branched-chain amino acids, per se.

The transport of branched-chain amino acids at the BRB was first described by Hjelle et al.[8] in 1978. They demonstrated that [^{3}H]L-leucine uptake by isolated retinal capillaries takes place in a concentration-dependent and Na^+-independent manner and is inhibited by L-valine and L-dihydroxyphenylalanine, suggesting that the amino acid transporter, system L, mediates L-leucine transport at the inner BRB. L-Leucine uptake into the retina has also been observed in vivo using the retinal uptake index method.[1] System L mediates the Na^+-independent transport of branched-chain and aromatic amino acids and L-type amino acid transporter 1 (LAT1/Slc7a5)[9] and LAT2 (Slc7a8)[10,11] have been shown to encode as system L. These transporters are unique because they require an additional protein, the heavy chain of 4F2 cell surface antigen (4F2hc/CD98/Slc3a2), for functional expression. The expression of LAT1 is localized in certain cells, such as brain capillary endothelial cells,[12–14] trophoblasts,[15] and corneal epithelial cells,[16] whereas LAT2 is expressed ubiquitously.[10,11] Recently, Nakauchi et al.[17] reported that LAT1, LAT2, and 4F2hc mRNA are expressed in a cultured human RPE cell line, an in vitro model of the outer BRB, although their contribution to amino acid transport has not yet been clarified. We previously reported[18] that 4F2hc mRNA is expressed in a conditionally immortalized rat retinal capillary endothelial cell line (TR-iBRB2 cells), which has been used as an in vitro model of the inner BRB,[19] and mediates L-cystine transport by combining with xCT. It presently remains unclear whether 4F2hc is involved in system L transport at the inner BRB. Consequently, our knowledge of the transport systems of branched-chain amino acids at the BRB, especially at the inner BRB, is still incomplete. It is important to elucidate the branched-chain amino acid transporter(s) at the inner BRB, since the inner two thirds of the human retina is nourished by a direct blood supply through the inner BRB.

We report evidence supporting the hypothesis that branched-chain amino acids in the retina are supplied from the

Investigative Ophthalmology & Visual Science, July 2005, Vol. 46, No. 7

circulating blood across the inner BRB. The characteristics and functions of L-leucine transport at the inner BRB were examined by in vivo integration plot analysis and using TR-iBRB2 cells. The localization of LAT1 at the inner BRB was determined by immunohistochemical analysis.

Materials and Methods

Animals

Male Wistar rats (250–300 g) and female Hartley guinea pigs (350–400 g) were purchased from SLC (Shizuoka, Japan). The investigations involving animals that are described in this report conformed to the provisions of the Animal Care Committee, Toyama Medical and Pharmaceutical University (no. 2003-48) and the ARVO Statement on the Use of Animals in Ophthalmic and Vision Research.

Blood-to-Retina [^{3}H]L-Leucine Transport Studies

The L-[4,5-^{3}H(*N*)]-leucine ([^{3}H]L-leucine, 42.5 Ci/mmol, PerkinElmer Life Science, Boston, MA) transport from the circulating blood to the retina was measured as described previously.[20,21] Briefly, the rats were anesthetized with an intramuscular injection of ketamine-xylazine (1.22 mg xylazine/kg and 125 mg ketamine/kg) and then [^{3}H]L-leucine (3 μCi/rat) was injected through the femoral vein. After collection of blood samples, rats were decapitated, and their retinas were removed. All samples were dissolved in 2 N NaOH and subsequently neutralized. The radioactivity was measured in a liquid scintillation counter (LS6500; Beckman-Coulter, Fullerton, CA). The apparent tissue-to-plasma concentration ratio (V_d) was used as an index of the tissue distribution characteristics of [^{3}H]L-leucine. This ratio [$V_d(t)$] (milliliters per gram of retina) was defined as the amount of [^{3}H] per gram of retina divided by that per milliliter plasma, calculated over the time-period of the experiment (t). The apparent influx permeability clearance of [^{3}H]L-leucine in the retina ($K_{in,retina}$) (microliters per minutes per gram of retina) was determined by integration plot analysis. In brief, $K_{in,retina}$ can be described by the following equation:

$$V_d(t) = K_{in,retina} \times AUC(t)/C_p(t) + V_i$$

where AUC(t) (dpm · minute per milliliter), $C_p(t)$ (dpm per milliliter), and V_i (milliliters per gram of tissue) represent the area under the plasma concentration time curve of [^{3}H]L-leucine from time 0 to t, the plasma [^{3}H]L-leucine concentration at time t, and the rapidly equilibrated distribution volume of [^{3}H]L-leucine, respectively.

Isolation of Rat Retinal Vascular Endothelial Cells

Magnetic beads coated with anti-rat CD31 antibodies were used to collect purified retinal vascular endothelial cells (RVECs), as described previously.[22] Briefly, mouse anti-rat CD31 antibodies (Chemicon, Temecula, CA) were incubated with Dynabeads pan-mouse IgG (Dynal Biotech, Lake Success, NY) overnight at 4°C to obtain magnetic beads coated with anti-rat CD31 antibodies. Rat retinas were minced and digested in 0.1% collagenase type I (Invitrogen, Carlsbad, CA) and 0.01% DNase I (Roche, Mannheim, Germany) in Ca^{2+}- and Mg^{2+}-free Hanks' balanced salt solution (HBSS) for 30 minutes at 37°C with agitation. Digests were filtered through a 30-μm nylon mesh and centrifuged at 200*g* for 10 minutes. The pellets were resuspended in Dulbecco's modified Eagle's medium (DMEM) containing 10% fetal bovine serum (FBS) and incubated with magnetic beads coated with anti-rat CD31 antibodies for 1 hour at room temperature. RVECs labeled with the magnetic beads were positively selected by affinity binding to the magnet.

Cell Culture

Primary cultured human retinal endothelial cells were obtained from Dainippon Pharmaceutical (Osaka, Japan) and cultured in endothelial cell basal medium containing growth supplement (Cell Applications, San Diego, CA) at 37°C. TR-iBRB2 cells were cultured in DMEM containing 10% FBS at 33°C. The permissive temperature for TR-iBRB2 cell culture is 33°C due to the presence of temperature-sensitive SV-40 large T-antigen.[19] All cells were seeded onto rat tail collagen type I–coated tissue culture plates (BD Biosciences, Bedford, MA) and cultured in a humidified atmosphere of 5% CO_2 and air.

Transport of [^{3}H]L-Leucine in TR-iBRB2 Cells

The [^{3}H]L-leucine uptake by TR-iBRB2 cells was measured according to a previous report.[21] Briefly, cells were incubated with 0.1 μCi [^{3}H]L-leucine (12 nM) in extracellular fluid (ECF) buffer consisting of 122 mM NaCl, 25 mM $NaHCO_3$, 3 mM KCl, 1.4 mM $CaCl_2$, 1.2 mM $MgSO_4$, 0.4 mM K_2HPO_4, 10 mM D-glucose and 10 mM HEPES (pH 7.4) at 37°C in the absence or presence of inhibitors. Na^+-free ECF buffers were prepared in two different ways: the choline ECF buffer was prepared by equimolar replacement of NaCl and $NaHCO_3$ with choline chloride and choline bicarbonate, respectively, whereas the Li ECF buffer was prepared by equimolar replacement of NaCl and $NaHCO_3$ with LiCl and $KHCO_3$, respectively. Cells were solubilized in 1 N NaOH and subsequently neutralized. An aliquot was taken for measurement of the radioactivity and protein content using, respectively, a liquid scintillation counter and a DC protein assay kit (Bio-Rad, Hercules, CA) with bovine serum albumin as a standard. The uptake of [^{3}H]L-leucine by TR-iBRB2 cells was expressed as the cell-to-medium ratio (microliters per milligram protein) as follows:

Cell-to-medium ratio = ([^{3}H] dpm in the cells per mg protein)/

([^{3}H] dpm in the medium per μL)

For kinetic studies, the Michaelis-Menten constant (K_m) and maximum rate (J_{max}) of L-leucine uptake were calculated from the equation, by using the nonlinear least-squares regression analysis program, MULTI.[23]

$$J = J_{max} \times C/(K_m + C)$$

where J and C are the uptake rate of L-leucine at 5 minutes and the concentration of L-leucine, respectively.

The 50% inhibition concentration (IC_{50}) for [^{3}H]L-leucine uptake by TR-iBRB2 cells was calculated by fitting the data to a sigmoidal inhibition model[21] using MULTI.[23]

$$J = J_0/[1 + ([I]/IC_{50})^n]$$

where J and J_0 are the uptake of [^{3}H]L-leucine in the presence and absence of inhibitors, respectively, [I] is the concentration of inhibitors and n is the Hill coefficient.

In the [^{3}H]L-leucine efflux studies, TR-iBRB cells were washed three times with ECF buffer and incubated with 0.1 μCi [^{3}H]L-leucine in ECF buffer for 5 minutes at 37°C to preload [^{3}H]L-leucine. Cells were then washed three times with ice-cold ECF buffer and incubated with ECF buffer in the absence or presence (control) of 2 mM amino acids at 37°C. After 4 minutes, incubated ECF buffer was taken to measure the efflux of preloaded [^{3}H]L-leucine from cells. The radioactivity in the cells was measured as just described. The efflux of [^{3}H]L-leucine by TR-iBRB2 cells was expressed as follows:

Fractional outflow(%) = ([^{3}H] dpm in the medium)/

([^{3}H] dpm in the cells+[^{3}H] dpm in the medium) × 100

Reverse Transcription–Polymerase Chain Reaction Analysis

Total cellular RNA was prepared using a kit (RNeasy; Qiagen, Hilden, Germany). Single-strand cDNA was made from total RNA by reverse transcription (RT) using an oligo dT primer. The polymerase chain

TABLE 1. Oligonucleotide Primers Used for PCR Amplification of cDNAs

Target mRNA	Accession Number	Upstream Primer (5′ to 3′)	Downstream Primer (5′ to 3′)	Product Size (bp)
LAT1 (Slc7a5)	NM_017353	CTC AAG CTC TGG ATC GAG CTG CTC	TTC CTG TAG GGG TTG ATC ATC TCC	440
LAT2 (Slc7a8)	NM_053442	CCT CGT CGC TCT GGC TTT CCT C	CGG GGG ATG TCA GGC TTC TTC CAG	558
4F2hc (Slc3a2)	NM_019283	CTC CCA GGA AGA TTT TAA AGA CCT TCT	TTC ATT TTG GTG GCT ACA ATG TCA G	141
β-Actin	NM_031144	TCA TGA AGT GTG ACG TTG ACA TCC GT	CCT AGA AGC ATT TGC GGT GCA CGA TG	285

reaction (PCR) was performed with LAT1, LAT2, or 4F2hc specific primers (Table 1) through 40 cycles of 94°C for 30 seconds, 60°C for 30 seconds, and 72°C for 1 minute. The PCR products were separated by electrophoresis on an agarose gel in the presence of ethidium bromide and visualized under ultraviolet light. The PCR products of the expected length were then cloned into a plasmid vector using a kit (p-GEM-T Easy Vector System I; Promega, Madison, WI) and amplified in *Escherichia coli*. Several clones were then sequenced from both directions using a DNA sequencer (Prism 310; Applied Biosystems Inc., [ABI] Foster City, CA).

Quantitative Real-Time PCR

Quantitative real-time PCR was performed on a sequence detector system (Prism 7700; ABI) with 2× SYBR Green PCR Master Mix (ABI) according to the manufacturer's protocol. To quantify the amount of specific mRNA in the samples, a standard curve was generated for each run using the plasmid (pGEM-T Easy Vector; Promega) containing the gene of interest. This enabled standardization of the initial mRNA content of cells relative to the amount of β-actin. The PCR was performed using LAT1-, LAT2-, or β-actin-specific primers (Table 1) and the cycling parameters are those given for RT-PCR.

Antibody Preparation

A peptide containing 13 amino acids of rat LAT1 (CRFKKPELERPIK, positions 424-435) was linked to maleimide-activated keyhole limpet hemocyanin (KLH; Pierce, Rockford, IL). The KLH-linked peptide (200 μg/injection) was emulsified by mixing with an equal volume of Freund's adjuvant (Difco, Detroit, MI) and injected subcutaneously into female Hartley guinea pigs at intervals of 2 weeks. Three weeks after the sixth injection, the immunoglobulin fraction was purified (HiTrap rProtein A FF column; Amersham Biosciences, Piscataway, NJ). Immunoglobulins specific to LAT1 peptide were affinity-purified (HiTrap NHS-activated HP column; Amersham Biosciences) carrying LAT1 peptide. Immunoblot analysis using rat brain extracts reported to express LAT1[12] showed that purified antibody strongly recognized a protein band at 40 kDa (Fig. 7; lane 1), the size of which is consistent with a previous report.[12] This band was abolished when purified immunoglobulins were preabsorbed with LAT1 antigen peptides (100 μg/mL; data not shown), indicating the specificity of the purified antibody for rat LAT1.

Immunoblot Analysis

Proteins were obtained by dissolving cells in sample buffer consisting of 5% sodium dodecyl sulfate (SDS), 250 mM Tris-HCl (pH 6.8), 10% glycerol, 6% 2-mercaptoethanol, and 0.01% bromophenol blue, followed by heating for 10 minutes at 95°C, and centrifugation for 10 minutes at 4°C and 9000*g*. Supernatants were separated and used as whole-cell extracts. Deglycosylation was performed by incubating the protein with *N*-glycosidase F (Roche). The protein (30 μg) was electrophoresed on an SDS-polyacrylamide gel and subsequently, electrotransferred to a polyvinylidene difluoride membrane. After incubation with blocking agent solution (Block Ace; Dainippon Pharmaceutical), the membranes were incubated with guinea pig polyclonal anti-LAT1 antibody (0.8 μg/mL) or goat polyclonal anti-4F2hc (CD98) antibody (1:300; Santa Cruz Biotechnology, Santa Cruz, CA) for 16 hours at 4°C. The membranes were subsequently incubated with horseradish peroxidase conjugated anti-guinea pig or goat IgG. The bands were visualized using an enhanced chemiluminescence kit (Amersham Biosciences).

Immunohistochemical Analysis

Under deep pentobarbital anesthesia (50 mg/kg body weight, intraperitoneally), rats were perfused transcardially with 4% formaldehyde in 0.1 M phosphate buffer. The eyeball was isolated and immersed in 0.5 M sucrose/HBSS solution. Sections (12 μm in thickness) were cut from the frozen eye with a cryostat (CM1900; Leica, Heidelberg, Germany) and mounted onto silanated glass slides (Dako, Carpinteria, CA). After incubation with 10% goat serum (Nichirei, Tokyo, Japan) for 1 hour at room temperature, sections were incubated with guinea pig polyclonal anti-LAT1 antibody (10 μg/mL) and rabbit polyclonal anti-GLUT1 antibody (1:500; Chemicon) for 36 hours at 4°C. Sections were subsequently incubated with FITC-conjugated anti-guinea pig and Cy3-conjugated anti-rabbit IgG antibodies (1:100; Chemicon) for 1 hour at room temperature. Sections were then mounted on coverslips using antifade mounting medium (Vectashield; Vector Laboratories, Burlingame, CA) and viewed using a confocal laser microscope (LSM 510; Carl Zeiss Meditec, Oberkochen, Germany).

Data Analysis

Unless otherwise indicated, all data represent means ± SEM. An unpaired, two-tailed Student's *t*-test was used to determine the significance of differences between two groups. Statistical significance of differences among means of several groups was determined by one-way analysis of variance followed by the modified Fisher's least-squares difference method.

RESULTS

L-Leucine Transport System at the Inner BRB

The in vivo blood-to-retina influx transport of L-leucine from the circulating blood to the retina through the BRB was evaluated by integration plot analysis after intravenous administration of [^{3}H]L-leucine to rats (Fig. 1). The $K_{in,retina}$ of [^{3}H]L-leucine was determined to be 203 ± 35 μL/(min · g retina) from the slope representing the apparent influx permeability clearance across the BRB. The apparent tissue-to-plasma concentration ratio (V_d) at 5 minutes was 1.88 ± 0.14 mL/g retina, far greater than that of [^{3}H]D-mannitol (0.058 mL/g retina at 15 minutes),[20] which is used as a nonpermeable paracellular marker. This result indicates that L-leucine is transported from the blood to the retina across the BRB.

Because the in vivo retinal uptake study represents L-leucine influx transport across both the inner and outer BRB, to determine the kinetic parameters of L-leucine and characterize L-leucine transport at the inner BRB, [^{3}H]L-leucine uptake and

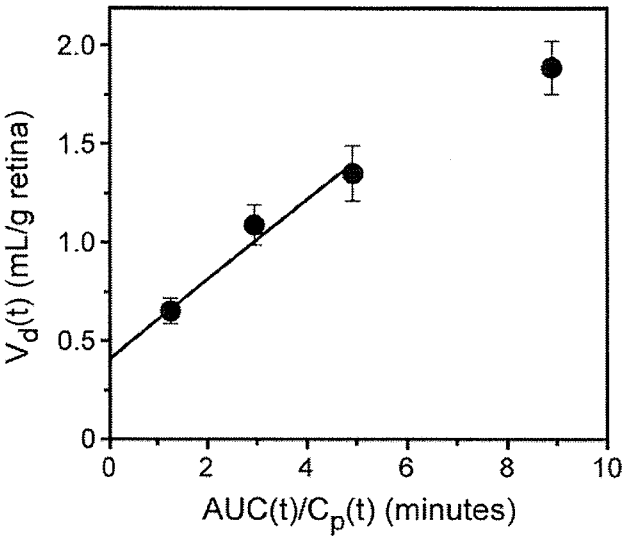

FIGURE 1. Integration plot of the initial uptake of [^{3}H]L-leucine by the retina after intravenous administration. [^{3}H]L-leucine (3 μCi/rat) was injected into the femoral vein. Each point represents the mean ± SEM (n = 3–5).

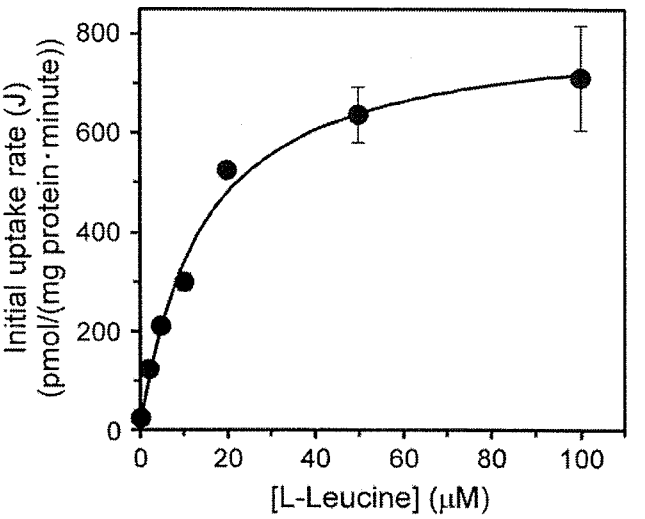

FIGURE 3. Concentration-dependence of L-leucine uptake by TR-iBRB2 cells. The [^{3}H]L-leucine (12 nM) uptake was performed at 5 minutes and 37°C. Each point represents the mean ± SEM (n = 4). The K_m is 14.1 ± 1.9 μM, and J_{max} is 819 ± 37 picomoles/(min · mg protein) (mean ± SD).

efflux studies were performed using TR-iBRB2 cells as an in vitro model of the inner BRB. The time-course of [^{3}H]L-leucine uptake by TR-iBRB2 cells is shown in Figure 2. [^{3}H]L-Leucine uptake increased linearly for 10 minutes, and the initial uptake rate was 20.1 μL/(min · mg protein). The inhibitory effect of Na^+-free conditions on [^{3}H]L-leucine uptake by TR-iBRB2 cells was examined under two different sets of conditions. Both choline ECF buffer and Li ECF buffer had little effect on [^{3}H]L-leucine uptake (94.2% ± 28.1% and 85.3% ± 14.1%, respectively; data not shown). This confirms that [^{3}H]L-leucine uptake by TR-iBRB2 cells is mediated by an Na^+-independent process.

Figure 3 shows the concentration-dependent uptake of L-leucine by TR-iBRB2 cells. The intracellular L-leucine uptake was saturable, and nonlinear least-squares regression analysis showed that the K_m and J_{max} were 14.1 ± 1.9 μM and 819 ± 37 picomoles/(min · mg protein) (mean ± SD), respectively.

The *cis* inhibition study was performed to characterize the [^{3}H]L-leucine uptake by TR-iBRB2 cells (Table 2). [^{3}H]L-Leucine uptake was inhibited by 2 mM L-leucine, L-phenylalanine, L-methionine, L-isoleucine, L-valine, L-tyrosine, and L-tryptophan, all of which are substrates of system L encoded by LAT1 or LAT2.[9–11] The system L-specific inhibitor, 2-aminobicyclo-(2,2,1)-heptane-2-carboylic acid (BCH) at a concentration of 2 mM strongly inhibited [^{3}H]L-leucine uptake. [^{3}H]L-Leucine uptake was also inhibited by more than 50% in the presence of substrates of LAT1, such as D-leucine, D-phenylalanine, and D-methionine, at a concentration of 2 mM.[9] However, it was only inhibited by 30% in the presence of substrates of LAT2, such as L-alanine and L-glutamine, at a concentration of 2 mM.[10,11] L-Glutamic acid, L-arginine, and L-proline had no effect

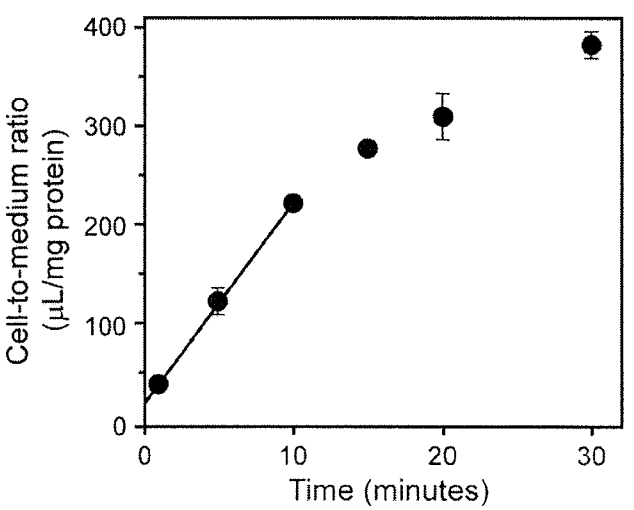

FIGURE 2. Time-course of [^{3}H]L-leucine uptake by TR-iBRB2 cells. The [^{3}H]L-leucine (12 nM) uptake was performed at 37°C. Each point represents the mean ± SEM (n = 4).

TABLE 2. Effect of Several Inhibitors on [^{3}H]L-Leucine Uptake by TR-iBRB2 Cells

Inhibitors	Percentage of Control
Control	100 ± 2
2 mM L-Leucine	2.88 ± 0.32*
2 mM L-Phenylalanine	20.0 ± 0.3*
2 mM L-Methionine	52.6 ± 1.8*
2 mM D-Leucine	45.7 ± 1.4*
2 mM D-Phenylalanine	39.7 ± 0.6*
2 mM D-Methionine	47.5 ± 1.9*
2 mM L-Isoleucine	36.5 ± 2.1*
2 mM L-Valine	46.9 ± 2.1*
2 mM L-Tyrosine	31.9 ± 0.2*
2 mM L-Tryptophan	17.3 ± 0.4*
2 mM L-Alanine	70.6 ± 4.4*
2 mM L-Glutamine	70.0 ± 2.3*
2 mM L-Glutamic acid	91.8 ± 5.8
2 mM L-Arginine	94.0 ± 3.3
2 mM L-Proline	87.5 ± 5.2
2 mM BCH	30.1 ± 0.8*
2 mM L-Dopa	42.1 ± 1.3*
2 mM Methyldopa	64.9 ± 1.3*
2 mM Gabapentin	79.6 ± 2.7*
100 μM Melphalan	58.4 ± 2.0*

[^{3}H]L-Leucine uptake (12 nM) was measured in the absence (control) or presence of inhibitors at 5 minutes and 37°C. Data are expressed as the mean ± S.E.M. (n = 4–24).

* $P < 0.01$, significantly different from the control.

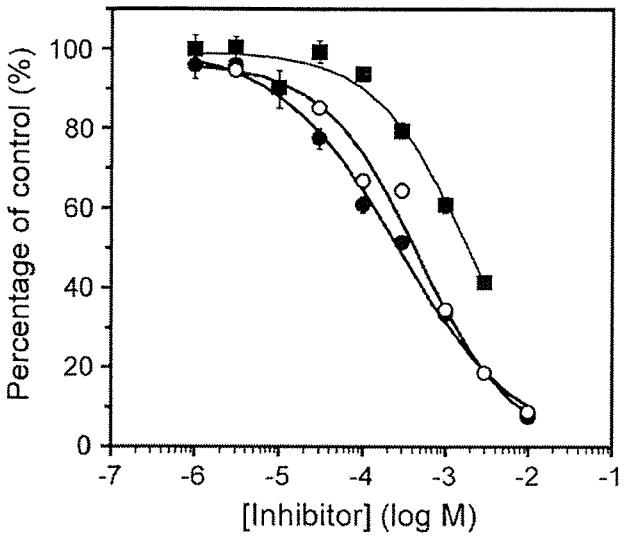

FIGURE 4. Concentration-dependent inhibition of amino acids involving the uptake of [^{3}H]L-leucine by TR-iBRB2 cells. [^{3}H]L-Leucine uptake (12 nM) was performed in the absence (control) or presence of various concentrations of L-phenylalanine (●), L-tyrosine (■), and L-tryptophan (○) at 5 minutes in 37°C. Each data point represents the mean ± SEM (n = 4). The IC_{50} was 266 ± 32 μM, 1.90 ± 0.18 mM, and 467 ± 93 μM for L-phenylalanine, L-tyrosine, and L-tryptophan, respectively (mean ± SD).

on [^{3}H]L-leucine uptake. In addition to naturally occurring amino acids, the amino acid-mimetic drugs 2 mM L-dopa, 2 mM methyldopa, 2 mM gabapentin, and 100 μM melphalan, significantly inhibited [^{3}H]L-leucine uptake by 58%, 35%, 20%, and 42%, respectively. These inhibitory characteristics of [^{3}H]L-leucine uptake by TR-iBRB2 cells are consistent with LAT1, rather than LAT2. In particular, L-phenylalanine, L-tyrosine, and L-tryptophan inhibited [^{3}H]L-leucine uptake in a concentration-dependent manner with an IC_{50} of 266 ± 32 μM, 1.90 ± 0.18 mM, and 467 ± 93 μM (mean ± SD), respectively (Fig. 4).

After preincubation of TR-iBRB2 cells with [^{3}H]L-leucine, the efflux of [^{3}H]L-leucine from TR-iBRB2 cells was measured in the absence or presence of extracellular amino acids. As shown in Figure 5, the efflux of [^{3}H]L-leucine from TR-iBRB2 cells was significantly stimulated by extracellular application of 2 mM L-leucine, L-phenylalanine, L-tryptophan, and BCH, whereas 2 mM L-arginine had no significant effect on [^{3}H]L-leucine efflux. These *trans*-stimulation effects by system L substrates are consistent with the view that system L functions as an exchanger.[24]

Expression of System L Transporters at the Inner BRB

To determine the mRNA expression at the in vivo inner BRB, RVECs were affinity purified from rat retinal homogenate by using magnetic beads coated with antibodies against CD31,[22] which is exclusively expressed on the membrane of endothelial cells. The magnetically collected and uncollected cells were isolated as the RVEC and non-RVEC fractions, respectively. The transcript levels of endothelial markers, such as CD31, Tie-2, claudin-5, occludin, and Jam-1, in the RVEC fraction were more than 100 times greater than those in the non-RVEC fraction.[22] RT-PCR analysis was performed to examine the expression of LAT1, LAT2, and 4F2hc in the rat brain as a positive control, rat retina, RVEC and non-RVEC fractions, and TR-iBRB2 cells. The bands of LAT1 and LAT2 were detected at 440 and 558 bp, respectively (Figs. 6A, 6B). The nucleotide sequence of the bands of TR-iBRB2 cells was identical with rat LAT1 and LAT2. 4F2hc was also expressed in all samples (Fig. 6C). To determine the dominant gene for system L at the inner BRB, quantitative real-time PCR analysis was performed to quantify the mRNA expression levels of LAT1 and LAT2 (Fig. 6D). The expression of LAT1 mRNA was 15 and 100 times greater than LAT2 mRNA in the RVEC fraction and TR-iBRB2 cells, respectively. Moreover, the expression level of LAT1 in the RVEC fraction was almost identical with that in the non-RVEC fraction, suggesting that the distribution of LAT1 is not restricted to the inner BRB. The expression of LAT2 in the RVEC fraction was 6.7-fold less than that in the non-RVEC-fraction. This result implies that LAT2 is not primarily distributed at the inner BRB of the rat retina.

The expression of LAT1 and 4F2hc protein was also determined in the rat retina, TR-iBRB2 cells, and primary cultured human retinal endothelial cells by immunoblot analysis, as shown in Figure 7. Rat brain was used as a positive control. The bands of LAT1 and 4F2hc were detected at 40 and 75 kDa, respectively, which are identical with the reported values.[12,25] Moreover, the band of 4F2hc shifted from 75 to 56 kDa in TR-iBRB2 cells after deglycosylation (Fig. 7B, lanes 5, 6), which is in agreement with the molecular mass of nonglycosylated rat 4F2hc predicted from its amino acid sequence (58 kDa). The localization of LAT1 in the rat retina was determined by immunohistochemical analysis (Fig. 8). Immunostaining of LAT1 (Figs. 8A, 8D, green) was observed along the retinal capillaries in the ganglion cell and inner plexiform layers and completely overlapped that of GLUT1 (Figs. 8B, 8E, red), which is known to be expressed in retinal capillaries.[6,7] LAT1 immunoreactivity was also detected in the ganglion cell and inner nuclear layers.

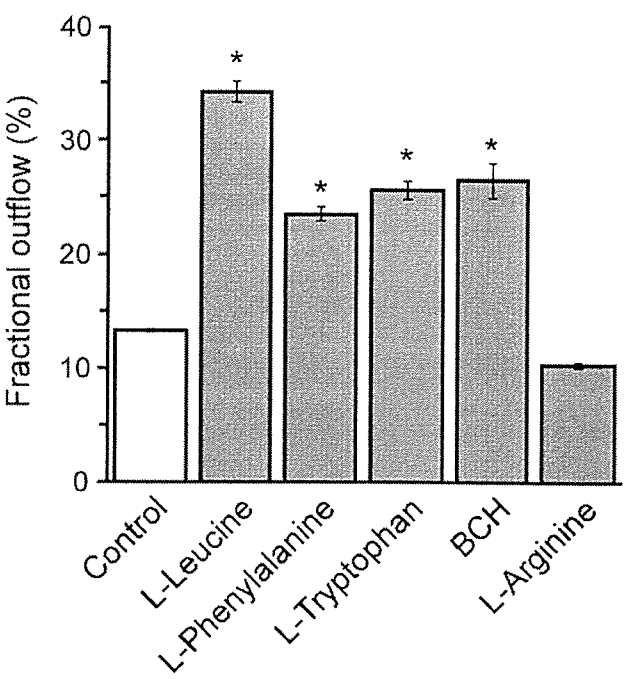

FIGURE 5. Effect of several amino acids on the efflux of [^{3}H]L-leucine from TR-iBRB2 cells. The efflux of preloaded [^{3}H]L-leucine was performed in the absence (control) or presence of extracellularly applied 2 mM L-leucine, L-phenylalanine, L-tryptophan, BCH, and L-arginine at 4 minutes in 37°C. Each column represents the mean ± SEM (n = 4). The fractional outflow (%) was 13.3 ± 0.2 (control), 34.2 ± 0.9 (L-leucine), 23.5 ± 0.6 (L-phenylalanine), 25.6 ± 0.8 (L-tryptophan), 26.5 ± 1.5 (BCH), and 10.3 ± 0.2 (L-arginine). *$P < 0.01$, significantly different from control.

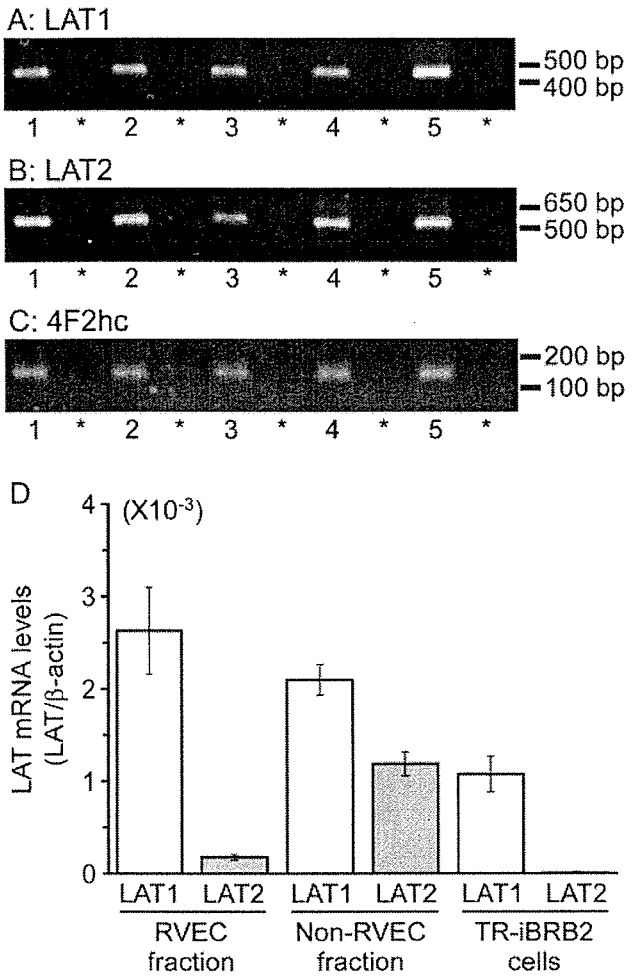

FIGURE 6. RT-PCR analysis of LAT1 (**A**), LAT2 (**B**), and 4F2hc (**C**) and the amount of LAT1 and LAT2 mRNA (**D**) in the RVEC fraction and TR-iBRB2 cells. (**A–C**) *Lane 1*: rat brain; *lane 2*: rat retina; *lane 3*: RVEC fraction; *lane 4*: non-RVEC fraction; *lane 5*: TR-iBRB2 cells. *Absence of reverse transcriptase relative to the respective *left* lane. Rat brain was used as a positive control. (**D**) The amount of LAT1 and LAT2 mRNAs were determined by quantitative real-time PCR analysis. Each column represents the mean ± SEM of at least three different samples. The quantity of LAT1 mRNA relative to β-actin mRNA (LAT1/β-actin) was (2.63 ± 0.47) × 10^{-3}, (2.10 ± 0.17) × 10^{-3}, and (1.08 ± 0.19) × 10^{-3}, and that of LAT2 mRNA (LAT2/β-actin) was (1.78 ± 0.31) × 10^{-4}, (1.19 ± 0.13) × 10^{-3}, and (1.02 ± 0.12) × 10^{-5} in the RVEC fraction, non-RVEC fraction, and TR-iBRB2 cells, respectively.

Such characteristic immunostaining of LAT1 was not seen after the use of preimmune guinea pig immunoglobulin (data not shown).

DISCUSSION

The present study demonstrates L-leucine transport from the circulating blood to the retina and provides the first evidence that LAT1 is localized in retinal capillary endothelial cells. Furthermore, the characteristics of [^{3}H]L-leucine influx and efflux transport in TR-iBRB2 cells used as an in vitro model of the inner BRB confirm that LAT1 is involved in L-leucine transport at the inner BRB.

[^{3}H]L-Leucine was transported from the blood to the retina across the BRB with a $K_{in,retina}$ of 203 ± 35 μL/(min · g retina) (Fig. 1), far greater than that of [^{14}C]sucrose (approximately 0.5 μL/(min · g retina), used as a nonpermeable paracellular marker.[26] This evidence suggests that L-leucine is transported by some carrier-mediated transport process, rather than by passive diffusion at the BRB. Although the estimated $K_{in,retina}$ reflects the transport across the inner and outer BRB, the presence of L-leucine transport at the inner BRB is strongly suggested by the fact that [^{3}H]L-leucine uptake occurs in TR-iBRB2 cells (Fig. 3). The K_m of 14.1 μM for [^{3}H]L-leucine uptake by TR-iBRB2 cells is in good agreement with that obtained for L-leucine uptake by rat LAT1 and 4F2hc expressed *Xenopus laevis* oocytes (K_m = 18 μM),[9] and different from that of rat LAT2 (K_m = 120 μM).[11] The K_m of L-leucine uptake by TR-iBRB2 cells is lower than the rat plasma concentration of L-leucine (84–160 μM).[27–29] In addition to L-leucine, LAT1 also prefers other branched-chain and aromatic amino acids such as L-phenylalanine and L-tyrosine circulating in the blood. These findings show that the inner BRB has the ability to supply L-leucine to the retina, although the LAT1-mediated amino acid transport at the inner BRB is saturated by substrate amino acids in the blood. In patients with phenylketonuria, the retinal concentration of LAT1-substrate amino acids, except phenylalanine, would be decreased by increasing the plasma concentration of phenylalanine relative to other amino acids, because of the competition for LAT1-mediated blood-to-retina transport between phenylalanine and other substrate amino acids. Children with phenylketonuria are reported to have impaired visual contrast sensitivity,[30] which is a behavioral measure sensitive to retinal dopamine levels, since reducing the concentration of a dopamine precursor, tyrosine, in phenylketonuria reduces the level of dopamine synthesis in the retina.

[^{3}H]L-Leucine uptake by TR-iBRB2 cells was Na^+-independent and inhibited by substrates and inhibitors of system L (Table 2). In particular, the degree of inhibition by substrates of LAT1,[9] D-leucine, D-phenylalanine, and D-methionine, was greater than that produced by the substrates of LAT2,[10,11] L-alanine and L-glutamate. System $b^{0,+}$, which is also an Na^+-independent transporter, mediates the transport of neutral and basic amino acids, such as L-leucine and L-arginine.[31] [^{3}H]L-Leucine uptake by TR-iBRB2 cells excludes the involvement of system $b^{0,+}$, since L-arginine produced no marked inhibition. However, the IC_{50} for L-phenylalanine (266 μM), L-tyrosine (1.90 mM), and L-tryptophan (467 μM) are large (Fig. 4), compared with the K_m for the transport of these amino acids via rat LAT1 (13 μM for L-phenylalanine and L-tyrosine and 19 μM for L-tryptophan).[32,33] Mouse LAT2 is also reported to exhibit

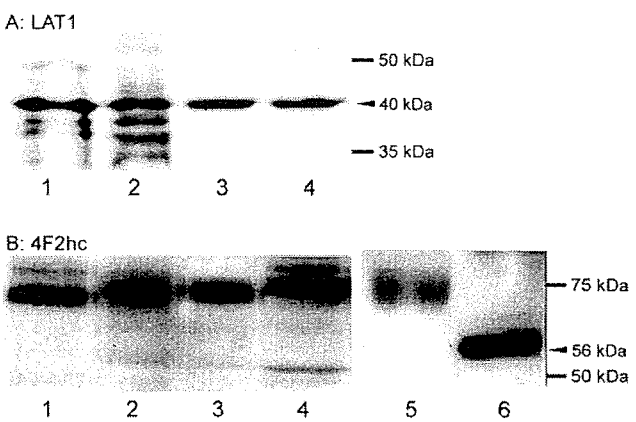

FIGURE 7. Immunoblot analysis of LAT1 (**A**) and 4F2hc (**B**). *Lane 1*: rat brain; *lane 2*: rat retina; *lane 3*: TR-iBRB2 cells; *lane 4*: primary cultured human retinal endothelial cells; *lane 5*: TR-iBRB2 cells without *N*-glycosidase F; *lane 6*: TR-iBRB2 cells with *N*-glycosidase F. Rat brain was used as a positive control.

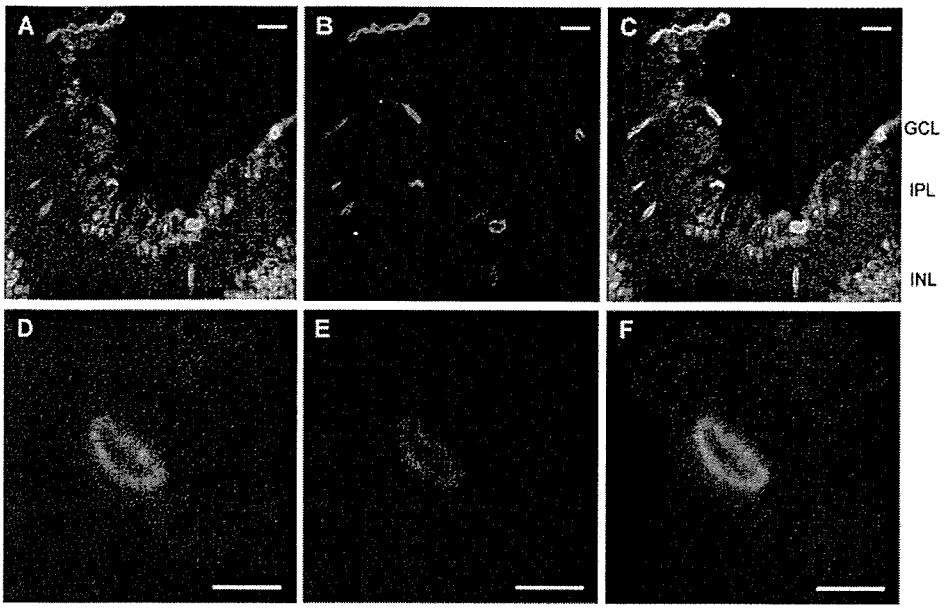

FIGURE 8. Localization of LAT1 in rat retinal capillary endothelial cells. The rat retina was stained with (A, D) anti-LAT1 antibody (*green*) and (B, E) anti-GLUT1 antibody (*red*). The images are merged in (C) and (F). LAT1 immunoreactivity was observed in retinal capillary endothelial cells as well as some other neural cells in the ganglion cell (GCL) and inner nuclear (INL) layers at lower magnification (A). Overlapped immunostaining of GLUT1 and LAT1 was observed at lower (C) and higher (F) magnifications. IPL, inner plexiform layer. Scale bar: (A–C) 20 μm; (D–F) 5 μm.

higher affinity transport for L-phenylalanine, with a K_m of 12 μM.[34] The corresponding kinetic parameters for rat LAT2-mediated transport of these amino acids have not been reported yet. Therefore, low- and high-affinity transport via LAT1 seems to take place in TR-iBRB2 cells, although nothing is presently known about the low-affinity process.

The efflux of [^{3}H]L-leucine from TR-iBRB2 cells was *trans*-stimulated by the extracellularly applied system L substrates, such as L-leucine, L-phenylalanine, L-tryptophan, and BCH (Fig. 5), supporting the view that LAT1 functions as an obligatory amino acid exchanger.[24] Therefore, LAT1 at the inner BRB requires intracellular substrate(s) to mediate the influx transport of L-leucine and other substrate amino acids from the blood. It has been reported that α-methylaminoisobutyric acid, which is a specific substrate of system A, is taken up in an Na^+-dependent manner into isolated bovine retinal capillaries,[35] suggesting that system A exists on the abluminal membrane of the inner BRB. At the blood–brain barrier, systems ASC, N, and A on the abluminal membrane mediate the Na^+-dependent uptake of neutral amino acids from the brain.[36–38] Although further studies are necessary to clarify the transport mechanism on the abluminal membrane of the inner BRB and identify neutral amino acids for the retina-to-blood efflux transport, the concentrative amino acid transport system(s) on the abluminal membrane accelerate the supply of intracellular substrates for LAT1 and the blood-to-retina transport of large neutral amino acids by LAT1 at the inner BRB.

Although the rat RVEC fraction and TR-iBRB2 cells express LAT1 and LAT2 mRNA (Figs. 6A, 6B), quantitative real-time PCR analysis clearly demonstrated that LAT1 is the main system L transporter in the RVEC fraction and TR-iBRB2 cells (Fig. 6D). Immunoblot analysis revealed that LAT1 protein is expressed in TR-iBRB2 cells and primary cultured human retinal endothelial cells (Fig. 7A), suggesting the expression of LAT1 at the inner BRB in rats as well as humans. Moreover, immunohistochemical analysis confirmed that LAT1 protein is localized in retinal capillary endothelial cells (Figs. 8A, 8D). The immunostaining image of LAT1 overlapped that of GLUT1 (Figs. 8C, 8F), which is known to be expressed in both the luminal and abluminal membranes of retinal capillary endothelial cells.[6,7] This observation is comparable with that at the blood–brain barrier, since LAT1 is reported to be localized at the luminal and abluminal membranes of brain capillary endothelial cells.[13] LAT1 immunoreactivity was also detected in other cells, especially in the inner nuclear layer (Fig. 8A), consistent with LAT1 mRNA expression in the non-RVEC fraction (Fig. 6D). Further studies are needed to identify those cells, apart from endothelial cells, expressing LAT1 in the retina. The expression of 4F2hc was also detected in the rat RVEC fraction, primary cultured human retinal endothelial cells, and TR-iBRB2 cells (Figs. 6C, 7B), as previously described for mRNA expression in TR-iBRB2 cells.[18] 4F2hc protein is reported to be a glycosylated protein[9] and the molecular weight of 4F2hc in TR-iBRB2 cells was reduced after deglycosylation treatment, indicating that 4F2hc in TR-iBRB2 cells is present as a glycosylated form. Taking these results into consideration, it appears that the heterodimer of LAT1 and 4F2hc is localized in retinal capillary endothelial cells and plays an important role in transporting L-leucine from the circulating blood to the retina across the inner BRB.

LAT1 mediates the transport of several essential amino acids, such as L-leucine, L-isoleucine, L-valine, L-histidine, L-methionine, L-phenylalanine, and L-tryptophan.[9] Therefore, LAT1-mediated essential amino acids must be supplied to the retina to synthesize retinal proteins. Moreover, LAT1-mediated branched-chain amino acids supplied to the retina are essential as nitrogen precursors of L-glutamate and GABA, which are the main excitatory and inhibitory neurotransmitters in the retina, respectively.[2,3] LAT1 also transports precursors of dopamine and serotonin, such as L-tyrosine and L-tryptophan. Dopamine is the main catecholamine in the retina and plays an essential role in the visual pathway as a neurotransmitter in amacrine and interplexiform cells.[39] Although serotonin synthesis in the retina has not been demonstrated, Chanut et al.[40] recently found that serotonin synthesis and its light–dark variation occur in the retina. Therefore, it is suggested that L-leucine supplied to the retina is converted to other retinal components, and then LAT1 at the inner BRB plays a physiological role in supplying precursors of proteins and neurotransmitters in the retina. Although the V_d of [^{3}H]L-leucine at 5 minutes (1.88 ± 0.14 mL/g retina) indicates that L-leucine uptake into the retina is apparently concentrative (Fig. 1), the leucine concentration in the rat retina (54 nanomoles/g retina)[41] is lower than that in rat plasma (84–160 μM).[27–29] This information implies that L-leucine supplied to the retina is converted to other retinal components. Moreover, it is speculated that the

impairment of LAT1 at the inner BRB limits neurotransmitter biosynthesis in the retina and markedly affects visual functions.

From a pharmacological viewpoint, LAT1 at the inner BRB could be useful for drug delivery into the retina. L-Dopa is the most widely used drug for Parkinson's disease, because L-dopa and its metabolite, 3-*O*-methyldopa, are transported through LAT1 at the blood–brain barrier.[12] [^{3}H]L-Leucine uptake by TR-iBRB2 cells is inhibited by 2 mM L-dopa and methyldopa (Table 2), supporting the possibility that L-dopa and methyldopa are transported by LAT1 at the inner BRB. Many patients with Parkinson's disease have blurred vision or other visual disturbances, which are reflected in the reduced retinal dopamine concentration and the delayed visual evoked potentials.[42] L-Dopa has been reported to reduce these delayed visual evoked potentials in Parkinson's disease.[43] Moreover, 2 mM gabapentin and 100 μM melphalan, neutral amino-acid–mimetic drugs, significantly inhibited [^{3}H]L-leucine uptake by TR-iBRB2 cells by 20% and 42%, respectively (Table 2). This result is consistent with the previous report that LAT1-mediated [^{3}H]L-phenylalanine transport is inhibited by gabapentin and melphalan with K_i of 340 and 49 μM, respectively.[33] Gabapentin has been shown to be an effective treatment in some patients with acquired pendular nystagmus.[44] Chemotherapy with melphalan is used in patients with retinoblastoma.[45] Therefore, it appears that LAT1 at the inner BRB plays a key role in transporting these drugs from the circulating blood to the retina and contributes to their pharmacological actions in the retina.

In conclusion, this is the first study to demonstrate the expression of LAT1 in retinal capillary endothelial cells. Although the responsible transporter for L-leucine at the inner BRB has remained unknown for a quarter of a century, we have now demonstrated that LAT1 is predominantly involved in blood-to-retina L-leucine transport at the inner BRB and seems to be closely involved in visual functions by supplying neurotransmitter precursors. These findings provide important information to improve our understanding of the physiological role of the inner BRB and drug delivery to the neural retina.

References

1. Törnquist P, Alm A. Carrier-mediated transport of amino acids through the blood-retinal and the blood-brain barriers. *Graefes Arch Clin Exp Ophthalmol.* 1986;224:21–25.
2. LaNoue KF, Berkich DA, Conway M, et al. Role of specific aminotransferases in *de novo* glutamate synthesis and redox shuttling in the retina. *J Neurosci Res.* 2001;66:914–922.
3. Lieth E, LaNoue KF, Berkich DA, et al. Nitrogen shuttling between neurons and glial cells during glutamate synthesis. *J Neurochem.* 2001;76:1712–1723.
4. Hosoya K, Tomi M. Advances in the cell biology of transport via the inner blood-retinal barrier: establishment of cell lines and transport functions. *Biol Pharm Bull.* 2005;28:1–8.
5. Cunha-Vaz JG. The blood-retinal barriers system: basic concepts and clinical evaluation. *Exp Eye Res.* 2004;78:715–721.
6. Fernandes R, Suzuki K, Kumagai AK. Inner blood-retinal barrier GLUT1 in long-term diabetic rats: an immunogold electron microscopic study. *Invest Ophthalmol Vis Sci.* 2003;44:3150–3154.
7. Takata K, Kasahara T, Kasahara M, Ezaki O, Hirano H. Ultracytochemical localization of the erythrocyte/HepG2-type glucose transporter (GLUT1) in cells of the blood-retinal barrier in the rat. *Invest Ophthalmol Vis Sci.* 1992;33:377–383.
8. Hjelle JT, Baird-Lambert J, Cardinale G, Specor S, Udenfriend S. Isolated microvessels: the blood-brain barrier in vitro. *Proc Natl Acad Sci USA.* 1978;75:4544–4548.
9. Kanai Y, Segawa H, Miyamoto K, et al. Expression cloning and characterization of a transporter for large neutral amino acids activated by the heavy chain of 4F2 antigen (CD98). *J Biol Chem.* 1998;273:23629–23632.
10. Pineda M, Fernandez E, Torrents D, et al. Identification of a membrane protein, LAT-2, that co-expresses with 4F2 heavy chain, an L-type amino acid transport activity with broad specificity for small and large zwitterionic amino acids. *J Biol Chem.* 1999;274:19738–19744.
11. Segawa H, Fukasawa Y, Miyamoto K, et al. Identification and functional characterization of a Na^+-independent neutral amino acid transporter with broad substrate selectivity. *J Biol Chem.* 1999;274:19745–19751.
12. Kageyama T, Nakamura M, Matsuo A, et al. The 4F2hc/LAT1 complex transports L-DOPA across the blood-brain barrier. *Brain Res.* 2000;879:115–121.
13. Matsuo H, Tsukada S, Nakata T, et al. Expression of a system L neutral amino acid transporter at the blood-brain barrier. *Neuroreport.* 2000;11:3507–3511.
14. Boado RJ, Li JY, Nagaya M, Zhang C, Pardridge WM. Selective expression of the large neutral amino acid transporter at the blood-brain barrier. *Proc Natl Acad Sci USA.* 1999;96:12079–12084.
15. Okamoto Y, Sakata M, Ogura K, et al. Expression and regulation of 4F2hc and hLAT1 in human trophoblasts. *Am J Physiol.* 2002;282:C196–C204.
16. Jain-Vakkalagadda B, Dey S, Pal D, Mitra AK. Identification and functional characterization of a Na^+-independent large neutral amino acid transporter, LAT1, in human and rabbit cornea. *Invest Ophthalmol Vis Sci.* 2003;44:2919–2927.
17. Nakauchi T, Ando A, Ueda-Yamada M, et al. Prevention of ornithine cytotoxicity by nonpolar side chain amino acids in retinal pigment epithelial cells. *Invest Ophthalmol Vis Sci.* 2003;44:5023–5028.
18. Tomi M, Hosoya K, Takanaga H, Ohtsuki S, Terasaki T. Induction of xCT gene expression and L-cystine transport activity by diethyl maleate at the inner blood-retinal barrier. *Invest Ophthalmol Vis Sci.* 2002;43:774–779.
19. Hosoya K, Tomi M, Ohtsuki S, et al. Conditionally immortalized retinal capillary endothelial cell lines (TR-iBRB) expressing differentiated endothelial cell functions derived from a transgenic rat. *Exp Eye Res.* 2001;72:163–172.
20. Nakashima T, Tomi M, Katayama K, et al. Blood-to-retina transport of creatine via creatine transporter (CRT) at the rat inner blood-retinal barrier. *J Neurochem.* 2004;89:1454–1461.
21. Hosoya K, Minamizono A, Katayama K, Terasaki T, Tomi M. Vitamin C transport in oxidized form across the rat blood-retinal barrier. *Invest Ophthalmol Vis Sci.* 2004;45:1232–1239.
22. Tomi M, Hosoya K. Application of magnetically isolated rat retinal vascular endothelial cells for the determination of transporter gene expression levels at the inner blood-retinal barrier. *J Neurochem.* 2004;91:1244–1248.
23. Yamaoka K, Tanigawara Y, Nakagawa T, Uno T. A pharmacokinetic analysis program (multi) for microcomputer. *J Pharmacobiodyn.* 1981;4:879–885.
24. Meier C, Ristic Z, Klauser S, Verrey F. Activation of system L heterodimeric amino acid exchangers by intracellular substrates. *EMBO J.* 2002;21:580–589.
25. Tomi M, Funaki T, Abukawa H, et al. Expression and regulation of L-cystine transporter, system x_c^-, in the newly developed rat retinal Müller cell line (TR-MUL). *Glia.* 2003;43:208–217.
26. Ennis SR, Betz AL. Sucrose permeability of the blood-retinal and blood-brain barriers: effects of diabetes, hypertonicity, and iodate. *Invest Ophthalmol Vis Sci.* 1986;27:1095–1102.
27. Doi M, Yamaoka I, Fukunaga T, Nakayama M. Isoleucine, a potent plasma glucose-lowering amino acid, stimulates glucose uptake in C2C12 myotubes. *Biochem Biophys Res Commun.* 2003;312:1111–1117.
28. Holecek M, Sprongl L, Tilser I. Metabolism of branched-chain amino acids in starved rats: the role of hepatic tissue. *Physiol Res.* 2001;50:25–33.
29. Araujo P, Wassermann GF, Tallini K, et al. Reduction of large neutral amino acid levels in plasma and brain of hyperleucinemic rats. *Neurochem Int.* 2001;38:529–537.
30. Diamond A, Herzberg C. Impaired sensitivity to visual contrast in children treated early and continuously for phenylketonuria. *Brain.* 1996;119:523–538.

31. Feliubadalo L, Font M, Purroy J, et al. Non-type I cystinuria caused by mutations in SLC7A9, encoding a subunit ($b^{0,+}$AT) of rBAT. *Nat Genet.* 1999;23:52–57.
32. Boado RJ, Li JY, Pardridge WM. Site-directed mutagenesis of rabbit LAT1 at amino acids 219 and 234. *J Neurochem.* 2003;84:1322–1331.
33. Uchino H, Kanai Y, Kim do K, et al. Transport of amino acid-related compounds mediated by L-type amino acid transporter 1 (LAT1): insights into the mechanisms of substrate recognition. *Mol Pharmacol.* 2002;61:729–737.
34. Rossier G, Meier C, Bauch C, et al. LAT2, a new basolateral 4F2hc/CD98-associated amino acid transporter of kidney and intestine. *J Biol Chem.* 1999;274:34948–34954.
35. Betz AL, Goldstein GW. Transport of hexoses, potassium and neutral amino acids into capillaries isolated from bovine retina. *Exp Eye Res.* 1980;30:593–605.
36. O'Kane RL, Vina JR, Simpson I, Hawkins RA. Na^+-dependent neutral amino acid transporters A, ASC, and N of the blood-brain barrier: mechanisms for neutral amino acid removal. *Am J Physiol.* 2004;287:E622–E629.
37. Takanaga H, Tokuda N, Ohtsuki S, Hosoya K, Terasaki T. ATA2 is predominantly expressed as system A at the blood-brain barrier and acts as brain-to-blood efflux transport for L-proline. *Mol Pharmacol.* 2002;61:1289–1296.
38. Tetsuka K, Takanaga H, Ohtsuki S, Hosoya K, Terasaki T. The L-isomer-selective transport of aspartic acid is mediated by ASCT2 at the blood-brain barrier. *J Neurochem.* 2003;87:891–901.
39. Frederick JM, Rayborn ME, Laties AM, Lam DM, Hollyfield JG. Dopaminergic neurons in the human retina. *J Comp Neurol.* 1982; 210:65–79.
40. Chanut E, Nguyen-Legros J, Labarthe B, Trouvin JH, Versaux-Botteri C. Serotonin synthesis and its light-dark variation in the rat retina. *J Neurochem.* 2002;83:863–869.
41. Pasantes-Morales H, Klethi J, Ledig M, Mandel P. Free amino acids of chicken and rat retina. *Brain Res.* 1972;41:494–497.
42. Bodis-Wollner I. Visual electrophysiology in Parkinson's disease: PERG, VEP and visual P300. *Clin Electroencephalogr.* 1997;28: 143–147.
43. Bhaskar PA, Vanchilingam S, Bhaskar EA, Devaprabhu A, Ganesan RA. Effect of L-dopa on visual evoked potential in patients with Parkinson's disease. *Neurology.* 1986;36:1119–1121.
44. Averbuch-Heller L, Tusa RJ, Fuhry L, et al. A double-blind controlled study of gabapentin and baclofen as treatment for acquired nystagmus. *Ann Neurol.* 1997;41:818–825.
45. Kaneko A, Suzuki S. Eye-preservation treatment of retinoblastoma with vitreous seeding. *Jpn J Clin Oncol.* 2003;33:601–607.

Available online at www.sciencedirect.com
SCIENCE DIRECT
Biochimica et Biophysica Acta 1758 (2006) 13–19
BIOCHIMICA ET BIOPHYSICA ACTA
BBA
http://www.elsevier.com/locate/bba

Functional and molecular characterization of adenosine transport at the rat inner blood–retinal barrier

Katsuhiko Nagase [a,b], Masatoshi Tomi [a], Masanori Tachikawa [a], Ken-ichi Hosoya [a,*]

[a] *Faculty of Pharmaceutical Sciences, University of Toyama, 2630, Sugitani, Toyama 930-0194, Japan*
[b] *Department of Hospital Pharmacy, School of Medicine, Kanazawa University, 13-1, Takara-machi, Kanazawa 920-8641, Japan*

Received 9 May 2005; received in revised form 6 December 2005; accepted 11 January 2006
Available online 2 February 2006

Abstract

The purpose of the present study was to characterize the adenosine transport system(s) at the inner blood–retinal barrier (inner BRB). A conditionally immortalized rat retinal capillary endothelial cell line (TR-iBRB2), used as an in vitro model of the inner BRB, expresses equilibrative nucleoside transporter 1 (ENT1), ENT2, concentrative nucleoside transporter 2 (CNT2), and CNT3 mRNAs. TR-iBRB2 cells exhibited an Na^+-independent and concentration-dependent [^{3}H]adenosine uptake with a Michaelis–Menten constant of 28.5 μM and a maximum uptake rate of 814 pmol/(min mg protein). [^{3}H]Adenosine uptake by TR-iBRB2 cells was strongly inhibited by 2 mM adenosine, inosine, uridine, and thymidine. On the other hand, this process was not inhibited by 100 nM nitrobenzylmercaptopurine riboside and dipyridamole. These uptake studies suggest that ENT2 is involved in [^{3}H]adenosine uptake by TR-iBRB2 cells. Quantitative real-time PCR revealed that the expression of ENT2 mRNA is 5.5-fold greater than that of ENT1 mRNA. An in vivo study suggested that [^{3}H]adenosine is transported from the blood to the retina and significantly inhibited by adenosine and thymidine. The results of this study show that ENT2 most likely mediates adenosine transport at the inner BRB and is expected to play an important role in regulating the adenosine concentration in the retina.

Keywords: Blood–retinal barrier; Adenosine; Nucleoside transporter

1. Introduction

Adenosine is an important intercellular signaling molecule and it plays a number of roles in retinal neurotransmission, blood flow, vascular development, and response to ischemia [1,2]. These effects are mediated through cell-surface adenosine receptors, so that the effect of adenosine in the retina is markedly influenced by the adenosine concentration in the retinal interstitial fluid. Most of the adenosine in the retinal interstitial fluid is thought to originate from the catabolism of adenosine monophosphate catalyzed by membrane-bound ecto-5′-nucleotidase (CD73) [1], which is localized in the innermost process of Müller cells [3]. Consequently, almost all of the retinal adenosine is distributed in the neighborhood of the innermost process of Müller cells in the ganglion cell layer, inner plexiform layer, and inner nuclear layer [4]. Retinal blood vessels are also distributed in ganglion cell layer, inner and outer plexiform layers, and inner nuclear layer [5] and form the inner blood–retinal barrier (inner BRB) which strictly regulates molecular transport between the blood and the retinal interstitial fluid [6]. Polska et al. [7] have reported that exogenous adenosine introduced via infusion increases the optic nerve head blood flow in healthy humans. Since adenosine in the blood needs to penetrate the inner BRB in order to activate its receptors expressed in vascular smooth muscle cells and increase blood flow, it has been suggested that adenosine transport system(s) at the inner BRB also have the ability to regulate the adenosine concentration in the retinal interstitial fluid and modulate retinal functions.

Two classes of nucleoside transporters have been described. The Na^+-independent equilibrative nucleoside transporter

Abbreviations: BRB, blood–retinal barrier; TR-iBRB2, conditionally immortalized rat retinal capillary endothelial cell line; NBMPR, nitrobenzylmercaptopurine riboside; ENT, equilibrative nucleoside transporter; CNT, concentrative nucleoside transporter; ECF, extracellular fluid; V_d, apparent retina-to-plasma concentration ratio; R_B, apparent blood-to-plasma concentration ratio; $K_{in,\ retina}$, apparent retinal uptake clearance of [^{3}H]adenosine; RUI, retinal uptake index; BBB, blood–brain barrier

* Corresponding author. Tel.: +81 76 434 7505; fax: +81 76 434 5172.
E-mail address: hosoyak@ms.toyama-mpu.ac.jp (K. Hosoya).

0005-2736/$ - see front matter © 2006 Elsevier B.V. All rights reserved.
doi:10.1016/j.bbamem.2006.01.011

(ENT) consists of ENT1 (Slc29a1) and ENT2 (Slc29a2) [8] while the Na^+-dependent concentrative nucleoside transporter (CNT) consists of CNT1 (Slc28a1), CNT2 (Slc28a2), and CNT3 (Slc28a3) [9]. They affect the concentration of adenosine available to its receptors in some organs. The inhibition of ENT1-mediated transport by the selective inhibitor, nitrobenzylmercaptopurine riboside (NBMPR), and consequent elevation of the adenosine concentration modulates glutamatergic synaptic transmission via presynaptic A_1 receptors in the superficial dorsal horn of the spinal cord in rats [10]. Moreover, the A_1 receptor-mediated chronotropic effect of adenosine is potentiated by the ENT1 inhibitor, dipyridamole, in the sinoatrial node of the guinea pig heart [11]. In the retina, it has been reported that [^{3}H]adenosine uptake and its inhibition by NBMPR take place in the retinal ganglion cell layer and inner nuclear layer of rabbits [12] and the cultured retinal neurons and photoreceptors of the chick embryo [13]. However, there is no information at all on the nucleoside transport system at the inner BRB although it would be very useful to have more information about adenosine transport mechanisms at the inner BRB in order to understand the regulation of the adenosine concentration in the neural retina.

The purpose of the present study was to elucidate the molecular mechanism of adenosine transport at the inner BRB. The characteristics and functions of adenosine transport at the inner BRB were examined using a conditionally immortalized rat retinal capillary endothelial cell line (TR-iBRB2) as an in vitro model of the inner BRB [14] and in vivo vascular injection techniques. TR-iBRB2 cells possess endothelial markers and glucose transporter 1 (GLUT1), P-glycoprotein, creatine transporter (CRT), and L-type amino acid transporter 1 (LAT1) [14–17], which are expressed at the inner BRB in vivo. Accordingly, TR-iBRB2 cells maintain certain in vivo functions and are a suitable in vitro model for the inner BRB.

2. Materials and methods

2.1. Animals

Male Wistar rats, weighing 250–300 g, were purchased from SLC (Shizuoka, Japan). The investigations using rats described in this report conformed to the provisions of the Animal Care Committee, Toyama Medical and Pharmaceutical University (currently University of Toyama) (#2003-48) and the ARVO Statement on the Use of Animals in Ophthalmic and Vision Research.

2.2. Cell culture

TR-iBRB2 cells were established from a transgenic rat harboring temperature-sensitive SV 40 large T-antigen gene [14]. TR-iBRB2 cells were seeded onto rat tail collagen type I-coated culture flasks (BD Biosciences, Bedford, MA). The cells were cultured in Dulbecco's modified Eagle's medium supplemented with 10% fetal bovine serum (Moregate, Bulimba, Australia) at 33 °C in a humidified atmosphere of 5% CO_2/air. The permissive temperature for TR-iBRB2 cell culture is 33 °C due to the presence of temperature-sensitive SV40 large T-antigen [14].

2.3. RT-PCR analysis

Total cellular RNA was prepared by using an Rneasy Kit (Qiagen, Hilden, Germany). Single-strand cDNA was made from total RNA by reverse transcription (RT) using oligo dT primer. The polymerase chain reaction (PCR) was performed with ENT1 (Slc29a1), ENT2 (Slc29a2), CNT1 (Slc28a1), CNT2 (Slc28a2), or CNT3 (Slc28a3) specific primers through 40 cycles of 94 °C for 30 sec, 60–62 °C for 30 sec, and 72 °C for 1 min. The sequences of the specific primers were as follows: the sense sequence was 5′-GCC AAC TAC ACA GCC CCC ATC A-3′ and the antisense sequence was 5′-TCA GCA GTC ACA GCA GGG AAC AA-3′ for rat ENT1 (GenBank accession number NM_031684), the sense sequence was 5′-CCT ACA GCA CCC TCT TCC TCA GT-3′ and the antisense sequence was 5′-CCC AGC CAA TCC ATG ACG TTG AA-3′ for rat ENT2 (GenBank accession number NM_031738) [18], the sense sequence was 5′-CAA CAC ACA GAG GCA AAG AGA GTC-3′ and the antisense sequence was 5′-CCA CAC CAG CAG CAA GGG CTA G-3′ for rat CNT1 (GenBank accession number NM_053863), the sense sequence was 5′-GGA AGA GTG ACT TGT GCA AGC TTG-3′ and the antisense sequence was 5′-GTG CTG GTA TAG AGG TCA CAG CA-3′ for rat CNT2 (GenBank accession number NM_031664), and the sense sequence was 5′-CTG TCT TTT GGG GAA TTG GAC TGC-3′ and the antisense sequence was 5′-CCA GTA GTG GAG ACT CTG TTT GC-3′ for rat CNT3 (GenBank accession number NM_080908). The PCR products were separated by electrophoresis on an agarose gel in the presence of ethidium bromide and visualized under ultraviolet light. The molecular identity of the resultant product was confirmed by sequence analysis using a DNA sequencer (ABI PRISM 310; Applied Biosystems, Foster City, CA).

2.4. [^{3}H]Adenosine uptake by TR-iBRB2 cells

The [2,8-^{3}H]adenosine ([^{3}H]adenosine, 35.9 Ci/mmol, Amersham Life Science, Buckinghamshire, UK) uptake by TR-iBRB2 cells was measured according to a previous report [15]. Briefly, TR-iBRB2 cells (1×10^5 cells/cm^2) were cultured at 33 °C for 48 hours on rat tail collagen type I-coated 24-well plates (BD Biosciences) and washed with 1 mL extracellular fluid (ECF) buffer consisting of 122 mM NaCl, 25 mM $NaHCO_3$, 3 mM KCl, 1.4 mM $CaCl_2$, 1.2 mM $MgSO_4$, 0.4 mM K_2HPO_4, 10 mM D-glucose and 10 mM HEPES (pH 7.4) at 37 °C. Uptake was initiated by applying 200 μL ECF buffer containing 0.1 μCi [^{3}H]adenosine (14 nM) at 37 °C in the presence or absence of inhibitors. Na^+-free ECF buffers were prepared by equimolar replacement of NaCl and $NaHCO_3$ with choline chloride and choline bicarbonate, respectively. After a predetermined period, uptake was terminated by removing the solution, and cells were immersed in ice-cold ECF buffer. The cells were then solubilized in 1 N NaOH and subsequently neutralized. An aliquot was taken for measurement of radioactivity and protein content using, respectively, a liquid scintillation counter (LS6500; Beckman-Coulter, Fullerton, CA) and a DC protein assay kit (Bio-rad, Hercules, CA) with bovine serum albumin as a standard.

For kinetic studies, the Michaelis–Menten constant (K_m) and maximum rate (J_{max}) of adenosine uptake were calculated from the following equation using the nonlinear least-square regression analysis program, MULTI [19].

$$J = J_{max} \times [S]/(K_m + [S]) \quad (1)$$

where $[S]$ and J are, respectively, the concentration of adenosine and the carrier-mediated component of the uptake rate of adenosine at 5 min estimated by subtracting the uptake rate in the presence of 10 mM non-radiolabeled adenosine, which represents a non-saturable component of the uptake rate.

2.5. Quantitative real-time PCR

Quantitative real-time PCR was performed using an ABI PRISM 7700 sequence detector system (Applied Biosystems) with 2× SYBR Green PCR Master Mix (Applied Biosystems) according to the manufacturer's protocol. To quantify the amount of specific mRNA in the samples, a standard curve was generated for each run using the plasmid (pGEM-T Easy Vector; Promega, Madison, WI) containing the gene of interest. This enabled standardization of the initial mRNA content of cells relative to the amount of β-actin. The PCR was performed using ENT1, ENT2, or β-actin-specific primers and the cycling parameters are those given above. The sequences of the specific primers of rat β-actin (GenBank accession number NM_031144) were as follows: sense, 5′-TCA TGA AGT GTG ACG TTG ACA TCC GT-3′ and antisense, 5′-CCT AGA AGC ATT TGC GGT GCA CGA TG-3′.